Anion-Initiated Trifluoromethylation by TMSCF3: Deconvolution of the Siliconate-Carbanion Dichotomy by Stopped-Flow NMR/IR

Anion-Initiated Trifluoromethylation by $TMSCF_3$: Deconvolution of the Siliconate-Carbanion Dichotomy by Stopped-Flow NMR/IR

Craig P. Johnston,[†∫] Thomas H. West,[†∫] Ruth E. Dooley,[†] Marc Reid,[†] Ariana B. Jones,[†] Edward J. King,[¥] Andrew G. Leach,[‡] and Guy C. Lloyd-Jones*[,†]

[†] EaStChem, University of Edinburgh, Joseph Black Building, David Brewster Road, Edinburgh, EH9 3FJ, UK

[‡] School of Pharmacy and Biomolecular Sciences, Liverpool John Moores University, Byrom Street, Liverpool, L3 3AF, UK

[¥] TgK Scientific Limited, 7 Long's Yard, St Margaret's Street, Bradford-on-Avon, BA15 1DH, UK

ABSTRACT: The mechanism of CF_3 transfer from R_3SiCF_3 (R = Me, Et, *i*Pr) to ketones and aldehydes, initiated by M^+X^- (<0.004 to 10 mol%) has been investigated by analysis of kinetics (variable-ratio stopped-flow NMR and IR), $^{13}C/^2H$ KIEs, LFER, addition of ligands (18-c-6, crypt-222), and density functional theory (DFT) calculations. The kinetics, reaction orders, and selectivity vary substantially with reagent (R_3SiCF_3) and initiator (M^+X^-). Traces of exogenous inhibitors present in the R_3SiCF_3 reagents, which vary substantially in proportion and identity between batches and suppliers, also affect the kinetics. Some reactions are complete in milliseconds, others take hours, others stall before completion. Despite these differences, a general mechanism has been elucidated in which the product alkoxide and CF_3^- anion act as chain carriers in an anionic chain reaction. Silyl enol ether generation competes with 1,2-addition and involves protonation of CF_3^- by the α-C–H of the ketone, and the OH of the enol. The overarching mechanism for trifluoromethylation by **1**, in which pentacoordinate siliconate intermediates are unable to directly transfer CF_3^- as a nucleophile or base, rationalizes why the turnover rate (per M^+X^- initiator) depends on the initial concentration (but not identity) of X^-, the identity (but not concentration) of M^+, the identity of the R_3SiCF_3 reagent, and the carbonyl / R_3SiCF_3 ratio. It also rationalizes which R_3SiCF_3 reagent effects the most rapid trifluoromethylation, for a specific M^+X^- initiator.

INTRODUCTION

The inclusion of fluorine-substituents in organic molecules is of pivotal importance to developments in, inter alia, pharmaceuticals,[1] agrochemicals,[2] electronics,[3] materials chemistry,[4] polymers,[5] synthesis,[6] and catalysis.[7] The transfer of a formally-nucleophilic CF_3-moiety to an electrophile is a preeminent method for the synthesis of trifluoromethylated compounds.[8] Conditions range from base-mediated reactions with fluoroform (CF_3H),[9] through to finely-tuned borazine-based CF_3-carriers recently reported by Szymczak.[10] In 1989, Ruppert reported that $TMSCF_3$ (**1a**)[11] undergoes addition to aldehydes and ketones in the presence of 10 mol% KF.[12] A faster process, using a soluble initiator ($Bu_4NF.xH_2O$; 0.6 mol%, 'TBAF') was reported soon after, by Prakash and Olah.[13] Acidic work-up affords the corresponding trifluoromethylated alcohols in good yield, Scheme 1.

Scheme 1. Trifluoromethylation of ketones / aldehydes.[12,13a]

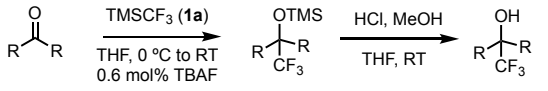

R = Ar, alkyl, vinyl, alkynyl, H

This mild and selective process[14] swiftly became adopted for the preparation of trifluoromethyl-carbinols,[15] including enantioselective additions involving enantiopure ammonium salts as initiators.[16] Indeed, over the last decade there has been an explosion of interest[17] in CF_3 transfer from $TMSCF_3$ (**1a**) to carbon (e.g. carbonyls,[14-17] imines,[18] vinylhalides[19] and aromatics[20]) and to heteroatoms such as sulfur-,[21] selenium-,[22] phosphorus-,[23] boron-,[24] iodine-,[25] and bismuth.[26] The formal loss of fluoride from CF_3 to facilitate electrophilic $TMSCF_2$-transfer,[27] or carbenoid CF_2-transfer,[28] has also been developed, as have numerous metal-mediated and catalyzed processes involving CF_3 derived from $TMSCF_3$ (**1a**).[29]

Despite anion-initiated trifluoromethylation by **1a** having become a mainstream synthetic method,[17-26] surprisingly little detail has emerged on the mechanism of CF_3 transfer, under the conditions of application, Scheme 1.[30] Various mechanistic dichotomies, including, inter alia, fluoride-initiation versus fluoride catalysis, and siliconate versus carbanion[23a] pathways, have been noted by Denmark,[30a] and by Reich;[30b] both of whom emphasize the lack of salient kinetic data.

Herein we report the first detailed study of the mechanism of anion-initiated CF_3 transfer from $TMSCF_3$ (**1a**) to ketone and aldehyde electrophiles.[12,17] The *in situ* NMR/IR investigations include analysis of reaction kinetics, selectivity, and side reactions, and the contrasting behaviour of homologues TES- (**1b**) and TIPS- (**1c**). Throughout the investigation, the kinetic studies have both informed, and been directed by,

density functional theory (DFT) analysis of proposed intermediates. What emerges is a nuanced kinetic landscape in which trifluoromethyl transfer proceeds via a carbanion pathway (CF_3^-), with the rate dictated by the identity of the electrophile, the concentration of the initiating anion, the identity of the initiator counter-cation, the electrophile / R_3SiCF_3 (**1**) concentration ratio, and the identity of the reagent (**1a**-**c**).

Scheme 2. Mechanisms (I–IV) for anion-induced trifluoromethylation of ketones using Ruppert's reagent (**1a**)[11] and homologues. L = 18-c-6, crypt-222. See text for full discussion.

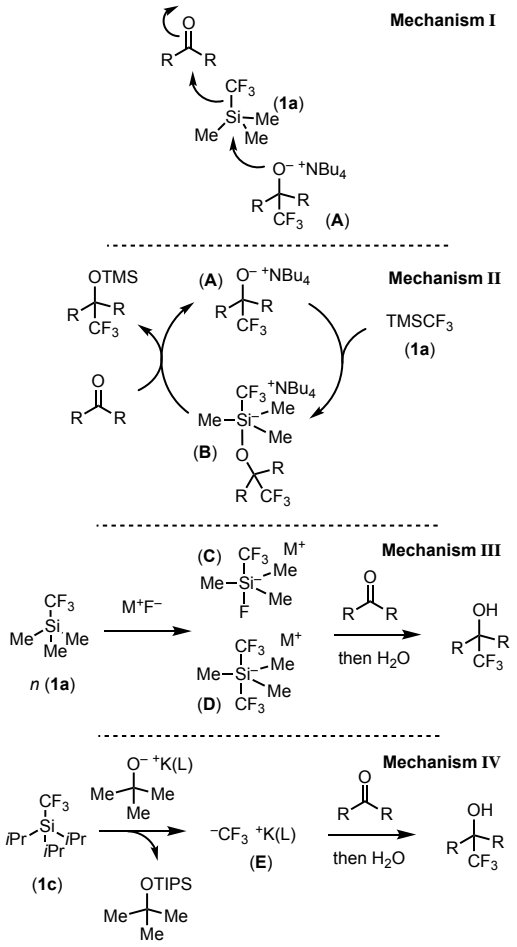

RESULTS AND DISCUSSION

1. Prior Studies. In early studies, a termolecular anionic chain-reaction (mechanism I, Scheme 2), was suggested for trifluoromethylation by **1a**.[13a] This was later expanded to a two-step process (mechanism II), where a pentacoordinate alkoxy-siliconate (**B**) delivers CF_3 to the ketone, and in doing so liberates the *O*-silylated product.[14] Mechanism II has been extensively adopted in the design and interpretation of asymmetric trifluoromethylation.[16,29,31]

In 1999, Naumann,[32] and Kolomeitsev and Röschenthaler[33] independently reported on the reaction of a range of soluble fluoride sources (e.g. $[Me_4N]^+F^-$) with $TMSCF_3$ (**1a**) at low temperature. Detailed ^1H, ^{13}C, ^{19}F and ^{29}Si NMR analysis identified the products as pentacoordinate complexes $[Me_3Si(F)(CF_3)]^-M^+$ (**C**) and $[Me_3Si(CF_3)_2]^-M^+$ (**D**). Both complexes decompose above –20 °C.[32,34] The speciation (**C** / **D**) is dependent on the stoichiometry (M^+F^- / **1a**), and the structure of **D** was confirmed by single crystal X-ray diffraction. Addition of cyclohexanone at –60 °C, followed by hydrolysis, afforded the corresponding trifluoromethylated alcohol, mechanism III.[32,35]

In 2014, Prakash[36] showed that the elusive[37] trifluoromethyl anion(oid)[38] can be detected *in situ* (^{13}C, ^{19}F NMR) at low temperatures after addition of KO*t*Bu / 18-crown-6 to **1a**. With the much bulkier reagent $TIPSCF_3$ (**1c**), the generation of ion-paired $[K(18\text{-c-}6)]^+[CF_3]^-$ (**E**) proceeds quantitatively at −78 °C over a period of 30 mins. Subsequent addition of PhCOMe (11 equiv.) or PhCHO (4 equiv.) afforded CF_3-addition products (22-68%) after quenching with H_2O, mechanism IV.[36] In 2015, Grushin[38] demonstrated that use of crypt-222 (L, Scheme 2) facilitates generation of the free CF_3^- carbanion; a THF solution-phase "noncovalently-bound ionic species".[38] The structure of the highly air- and temperature-sensitive salt, $[K(crypt\text{-}222)]^+[CF_3]^-$ (**E**), was confirmed by single crystal X-ray diffraction.[38,39]

The pioneering studies summarized above have been highly enlightening regarding the structure and stability of pentacoordinate (trifluoromethyl)siliconates (**C**, **D**),[32,33] and their ability to release the trifluoromethane anion(oid) (**E**) under specific conditions.[36,38] However, they do not yield direct detail on the kinetics and mode of transfer of CF_3 from $TMSCF_3$ (**1a**) to a carbonyl electrophile, using a catalytic fluoride-based initiator (M^+X^-), at ambient temperature.[12,13]

2. Preliminary Investigations. We began by study of the reaction of $TMSCF_3$ (**1a**) with aldehydes and ketones in THF, chlorobenzene, and DMF. After addition of catalytic quantities (0.1 to 1 mol%) of TBAF, ^{19}F NMR readily facilitated analysis of the proportions of residual reagent (**1a**) and the [1,2]-addition products. The reaction of 4-fluoroacetophenone (**2**) in THF at ambient temperatures proved ideal, the additional ^{19}F nucleus allowing simultaneous analysis of reagent (**1a**; 0.48 M), substrate (**2**; 0.40 M), and product ($\mathbf{3}_{OTMS}$), Scheme 3.

Scheme 3. Trifluoromethylation of ketone **2** (Ar = 4-F-C_6H_4).

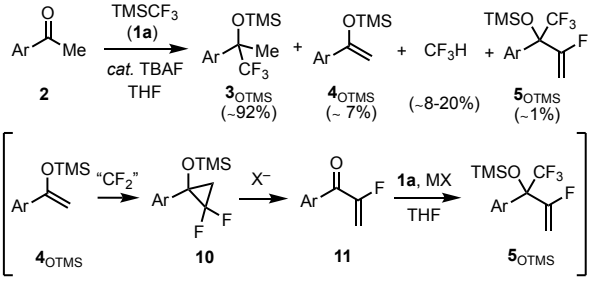

Reactions were assembled manually in 5 mm NMR tubes in the glove box prior to analysis *in situ* by ^{19}F NMR. Three side-products were identified: fluoroform (CF_3H), the silylenol ether ($\mathbf{4}_{OTMS}$) and a homologated addition product $\mathbf{5}_{OTMS}$. Reactions conducted in d_8-THF proceeded analogously, and generated CF_3H, not CF_3D.[40] The identity of $\mathbf{5}_{OTMS}$, which was confirmed by independent synthesis, is consistent with difluorocyclopropanation of silylenol ether $\mathbf{4}_{OTMS}$ to generate **10**, followed by a known[41] anion-induced ring-opening elimination to give fluoroenone **11**, and subsequent 1,2-selective[12]

trifluoromethylation. Addition of independently synthesized[42] **10** to the reaction (Scheme 3) generated **5**$_{OTMS}$.

Reaction rates, and extent of fluoroform generation (Scheme 3), were found to vary significantly between batches of TBAF (1 M, THF, ~5 wt% H_2O). Replacing TBAF with anhydrous $[Bu_4N][Ph_3SiF_2]$ ('TBAT')[43] gave more reproducible data. However, the fast turnover precluded detailed kinetic analysis; this aspect was addressed using stopped-flow methods, *vide infra*. Nonetheless, ^{19}F NMR analysis revealed that CF_3H is liberated in two distinct phases. The first is an initial burst of extremely rapid CF_3H generation, and arises from TBAT-catalyzed reaction of $TMSCF_3$ (**1a**) with traces of adventitious water.[44] The second phase of CF_3H generation proceeds in concert with reaction of the ketone (**2**) and directly correlates with the rate of generation of silylenol ether (**4**$_{OTMS}$), as confirmed by ^2H-labelling (d_3-**2** → CF_3D + d_2-**4**$_{OTMS}$). The selectivity (**3**$_{OTMS}$ versus **4**$_{OTMS}$) is discussed later.

3. Stability, Inhibition, and Tests for Radicals. The stability of the reaction system after complete consumption of the limiting reagent (ketone **2** or $TMSCF_3$ **1a**) was found to depend on which one was in excess. Reactions in which **2** was in excess, underwent turn-over on addition of further $TMSCF_3$ **1a**, even after a period of many hours. In contrast, for reactions where **1a** was in excess, additional **2** had to be added within a few minutes to fully reinstate turnover (see SI); consistent with the known instability of pentacoordinate (trifluoromethyl)siliconates, e.g **C** and **D**, at ambient temperatures.[32-34] Further tests established that the reactions were not sensitive to exogenous water *per se*, as they rapidly self-dehydrated via generation of CF_3H + hexamethyldisiloxane, prior to reaction of the ketone (**2**).[45] The rates were unaffected by visible light, by exogenous product (**3**$_{OTMS}$), and by CF_3H. Deliberate sparging of the normal reaction mixture (**1a** / **2** / TBAT 0.15 mM, 0.038 mol%, THF, Scheme 3) with air caused complete inhibition of turnover, but only when a sufficient volume of CO_2 (~400 ppm) had been added to convert the active anion(s) into trifluoroacetate (i.e. $[Bu_4N][CF_3CO_2]$, detected by ^{19}F NMR). Separate controls confirmed that the rate of trifluoromethylation is unaffected by CO_2-scrubbed air, and that $[Bu_4N][CF_3CO_2]$ is not effective as an initiator.

Scheme 4. Tests for radical intermediates.

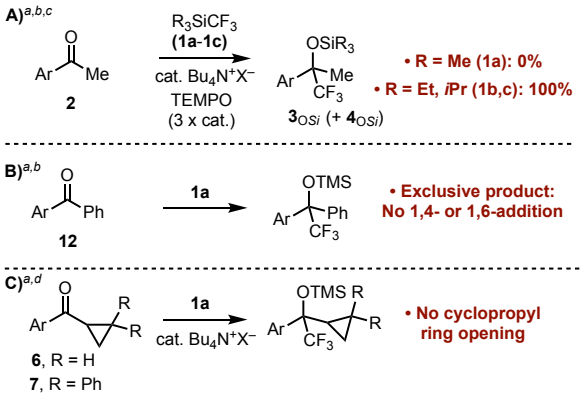

[a](Ar = 4-F-C_6H_4); ketone (**2**, **6**, **7**, **12**, 0.40 M), **1a-c** (0.48 M), THF, 21 °C. [b]TBAT (0.04 mol%, 0.15 mM), [c]TEMPO (0.12 mol%, 0.45 mM; up to 80 mM with **1b**,**c**). [d]TBAF (4 mM, 1 mol%).

However, the reactions were inhibited by addition of the persistent radical, TEMPO. Indeed, just 0.45 mM TEMPO induced complete inhibition of the reaction of **1a** with **2**, initiated by 0.15 mM TBAT (Scheme 4, A). In contrast, TEMPO had negligible impact on reactions employing TES (**1b**) and TIPS (**1c**), even when present at much higher concentrations (80 mM TEMPO); the origins of this profound difference in behavior is discussed later. Nonetheless, further tests for discrete radical intermediates[46,47] were conclusively negative: 4-F-benzophenone (**12**) exclusively underwent 1,2-addition (Scheme 4, B),[48,49] cyclopropyl ketones (**6**/**7**) reacted without any trace of competing ring-opening[50] (Scheme 4, C), and competition between ketone **2** and 4-biphenyl methylketone for limiting $TMSCF_3$ (**1a**) favored **2** (k_{rel} = 1.93).[51]

4. General Effects of Initiator on Rate and Selectivity. A range of initiators (M^+X^-) were tested and found to strongly impact the reaction outcome. In the majority of cases, the reactions initiated 'instantly' and the identity of X^- had no influence on the rate[52] or selectivity (**3**$_{OTMS}$ / **4**$_{OTMS}$). Specific effects were found to be dictated by the identity of the counter-cation (M^+), Table 1.

Table 1. Examples of effect of initiator M^+ and reagent (**1a-c**) on selectivity (**3**$_{OSi}$ /**4**$_{OSi}$) and rate of trifluoromethylation of **2**.

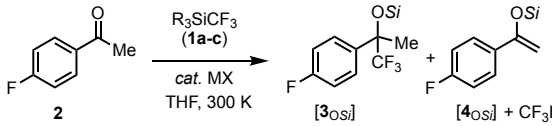

M^+	$[M^+X^-]_0$ mM	TMS **1a** **3**/**4**[a] (time)[b]	TES **1b** **3**/**4**[a] (time)[b]	TIPS **1c** **3**/**4**[a] (time)[b]
$[Bu_4N]^+$	1.5	12 / 1 (<90 s)	1.5 / 1 (<90 s)	1 / 1 (30 min.)
$[K]^+$	0.15	36 / 1 (<90 s)	3.0 / 1[c] (30 min.)	NR
$[K(L)]^+$ [d]	1.5	6.6 / 1 (6 min.)	2.4 / 1 (<90 s)	1 / 1 (3.6 min.)

[a]Selectivity **3**$_{OSi}$/(**4**$_{OSi}$+CF_3H) measured *in situ* by ^{19}F NMR after manual assembly in an NMR tube; selectivity is independent of X^-. [b]times indicated are for >97% conversion of **2**, at 300 K. [c]85% conversion. [d] $[K(L)]^+$ = K(crypt-222)]$^+$, generated *in situ* from KOPh + crypt-222.

Reactions where M^+ = K^+, Cs^+ proceeded rapidly to completion, with higher selectivity for **3**$_{OTMS}$ / **4**$_{OTMS}$ compared to Bu_4N^+. Reactions stalled when the cation was Li^+ or Na^+.[53] For the K^+-mediated system, the rate was strongly attenuated by addition of 18-crown-6, or crypt-222, with the latter causing turnover to become slower and less selective (**3**$_{OTMS}$ / **4**$_{OTMS}$) than reactions initiated by TBAT (counter-cation Bu_4N^+). The identity of M^+ was also found to affect the degree of charge-development (ρ ranging from 1.8 to 3.0) in the ketone (R = Me, Scheme 5) at the product-determining transition state for CF_3 transfer. Benzaldehydes (R = H) behaved analogously.

Scheme 5. Effect of initiator M^+ on reaction constant (ρ).

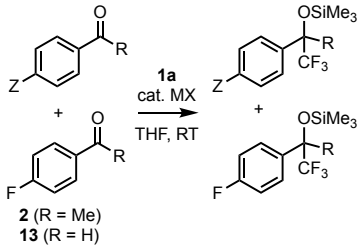

M^+	$\rho_{(Me)}$	$\rho_{(H)}$
Na	1.76	--
K	1.79	1.27
Cs	2.00	--
K(18-c-6)	2.00	2.01
NBu_4	2.62	2.35
K(crypt-222)	2.98	2.55

$\rho = \sigma\log_{10}(k_Z/k_F)$ [^{19}F NMR]

[a] i) 4-Z-C_6H_4COR (0.2 M), **2**/**13** (0.2 M), **1a** (0.04 M), PhF (0.4 M), MX (0.00015 M; 0.038 mol%). Z = Ph, OMe, CF_3, Me, Br. Hammett rho values calculated from product ratios, see SI.

5. Effect of Silyl Reagent on Rate and Selectivity. To further probe the CF_3 transfer process, we compared $TMSCF_3$ (**1a**) with $TESCF_3$ (**1b**) and $TIPSCF_3$ (**1c**), Table 1. The effects of changing the reagent were counter-intuitive and initially misleading regarding the mechanism of CF_3 transfer, *vide infra*. Reactions employing $TESCF_3$ (**1b**) gave lower selectivity (**3**$_{OTES}$ / **4**$_{OTES}$ ≈ 1.5 / 1) and proceeded very rapidly, even at low TBAT concentrations (150 μM, 0.0375 mol%; below this, reactions failed to initiate). In contrast, reactions employing $TIPSCF_3$ (**1c**) proceeded very slowly, requiring high initiator concentrations to proceed efficiently (> 1.5 mM, 0.375 mol%) and gave even lower selectivity (**3**$_{OTIPS}$ / **4**$_{OTIPS}$ ≈ 1 / 1).

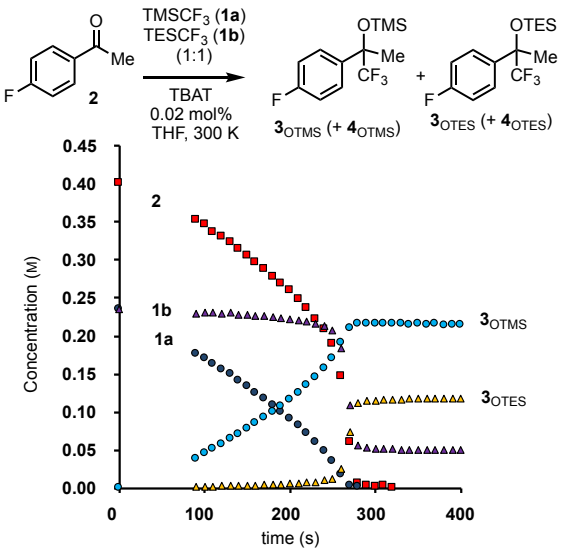

Figure 1. Competition between $TMSCF_3$ (**1a**) / $TESCF_3$ (**1b**); see text for full discussion. Reaction conditions: **2** (0.4 M), **1a** (0.24 M), **1b** (0.24 M), PhF (internal standard, 0.4 M), TBAT (75 μM, 0.019 mol%); ^{19}F NMR analysis, manual assembly.

Further insight was afforded by reaction of a 50/50 mixture of $TMSCF_3$ (**1a**) and $TESCF_3$ (**1b**), initiated by TBAT (75 μM, 0.019 mol%), Figure 1. The first 4 minutes of reaction is dominated by turnover of $TMSCF_3$ (**1a**) to generate **3**$_{OTMS}$/**4**$_{OTMS}$ and upon near-complete consumption of **1a**, turnover accelerates substantially as the $TESCF_3$ (**1b**) is engaged to generate **3**$_{OTES}$/**4**$_{OTES}$.The data indicate that the less-hindered reagent (**1a**) monopolizes the anion, but undergoes slower turnover.

Under conditions where anion-induced reactions of TMS (**1a**), TES (**1b**) and TIPS (**1c**) with **2** could be conducted slowly enough to be accurately monitored *in situ* by ^{19}F NMR, the ratios of enol / addition product (**4**$_{OSi}$ / **3**$_{OSi}$) were all *constant* throughout the reaction evolution, Figure 2. A further distinction originated from the impact of the addition of crypt-222 to KOPh-initiated reactions. As noted above, for $TMSCF_3$ (**1a**) the incarceration of the K^+ in the crypt-222 ligand substantially attenuates the rate and selectivity. In stark contrast, for $TIPSCF_3$ (**1c**), turnover is substantially *accelerated* by addition of crypt-222 to inhibit K^+ / anion pairing.

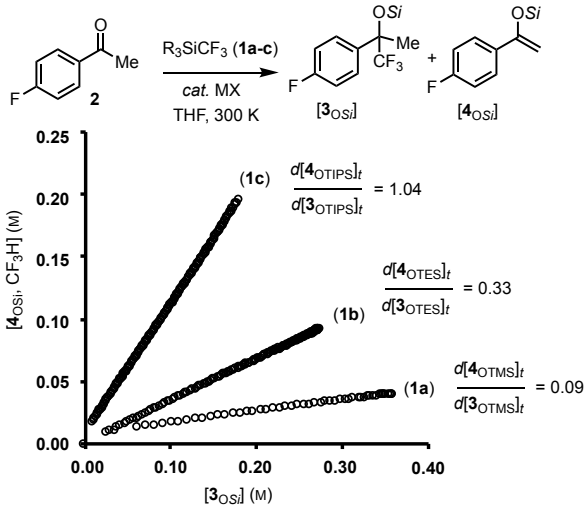

Figure 2. Constant-ratio of $[\mathbf{4}_{OSi}]_t$ / $[\mathbf{3}_{OSi}]_t$. Conditions: **2** (0.4 M), **1a-c** (0.48 M), PhF (internal standard, 0.4 M), MX (TBAT 150 μM for **1a**; KOPh 0.15 mM for **1b**, TBAT 1.5 mM for **1c**).

Reactions with labelled ketone (aryl-d_4-**2**; CD_3-**2**; ^{13}CO-**2**) were also instructive, Table 2. Reaction of $TMSCF_3$ (**1a**) with **2** initiated by TBAT (0.15 mM) proceeds with a very low ^{13}C kinetic isotope effect (KIE), determined by competition with aryl-d_4-**2**, after normalizing for the effect of aryl deuteration.

Table 2. KIEs and ^{2}H-exchange in the reaction of ketone **2**[a,b]

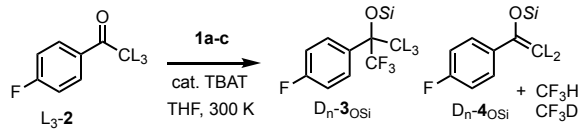

CL_3 (reagent)	1a-c	2, $\mathbf{3}_{OSi}$	k_H / k_D	
CH_3 (^{13}C=O)	$TMSCF_3$ (**1a**)	CH_3	–	(k_{12C}/k_{13C} = 1.008)[c]
CH_3 (C_6D_4)	$TMSCF_3$ (**1a**)	CH_3	1.038[d]	
CD_3	$TMSCF_3$ (**1a**)	CD_3	6.4	(**3**/**4**$_{OTMS}$ = 72 / 1)
CD_3 + CH_3	$TMSCF_3$ (**1a**)	CD_3 / CH_3 only	6.1	(rate: CF_3H/CF_3D)
CD_3	$TESCF_3$ (**1b**)	CD_3	3.1	(**3**/**4**$_{OTES}$ = 4.3 / 1)
CD_3 + CH_3	$TESCF_3$ (**1b**)	partial CD_{3-n}/H_n	–	(**3**/**4**$_{OTES}$ = 2.3 / 1)
CD_3	$TIPSCF_3$ (**1c**)	CD_3	1.1	(**3**/**4**$_{OTIPS}$: 1.1 / 1)
CD_3 + CH_3	$TIPSCF_3$ (**1c**)	full CD_{3-n}/H_n	1.0	(rate: CF_3H/CF_3D)

[a] Ketone (**2** / ^{2}H$_3$-**2**; 0.40 M), **1a-c** (0.48 M), THF, 300 K. TBAT (0.04 mol%, 0.15 mM), [b] Selectivity **3**$_{OSi}$/(**4**$_{OSi}$ + CF_3H/D) and exchange measured *in situ* by ^{19}F NMR analysis. [c] KIE determined by competition with *aryl*-d_4-**2**. [d] ^{2}HKIE induced by aryl-deuteration, determined by competition with unlabelled **2**.

In contrast, a substantial primary ^{2}H KIE, determined from [CF_3D] versus [d_3-**3**$_{OSi}$], as in Figure 2, increases the addition / enol selectivity (k_H/k_D = 6.4). Reactions of mixtures of **2** and d_3-**2** proceeded with no detectable scrambling of D/H between **2** / D_3-**2** during turnover, provided that [**1a**]$_0$ > [**2**]$_0$, and again proceeded with a high KIE (k_H/k_D = 6.1). With $TESCF_3$ (**1b**) a moderate KIE (k_H/k_D = 3.1) was observed, with a trace of D/H exchange between **2** and D_3-**2** on co-reaction, and thus into products d_n-**3**/d_n-**4**. With $TIPSCF_3$ (**1a**) there was no significant KIE and a statistical mixture of isotopologues of d_n-**2/3** (n = 0–3) was evident immediately after initiation of the reaction.[54]

6. Variable-Ratio Stopped-Flow NMR and IR. Detailed exploration of the kinetics of the trifluoromethylation by **1a** required techniques for rapid acquisition of kinetic data (some systems had formal turnover frequencies well in excess of 5,000 s^{-1}, *vide infra*) in a time- and material-efficient manner. Stopped-flow techniques are ideal for rapid and reproducible initiation and analysis of these reactions. However, the classic fixed-ratio dual input mode of operation (*A* + *B*; Figure 3a) requires separate solutions to be prepared for every variation in conditions. For a three-component process such as R_3SiCF_3 (**1**) + ketone **2** + initiator (M^+X^-), a very large number of stock solutions are required to study reactions with different concentrations of reactants and initiator.

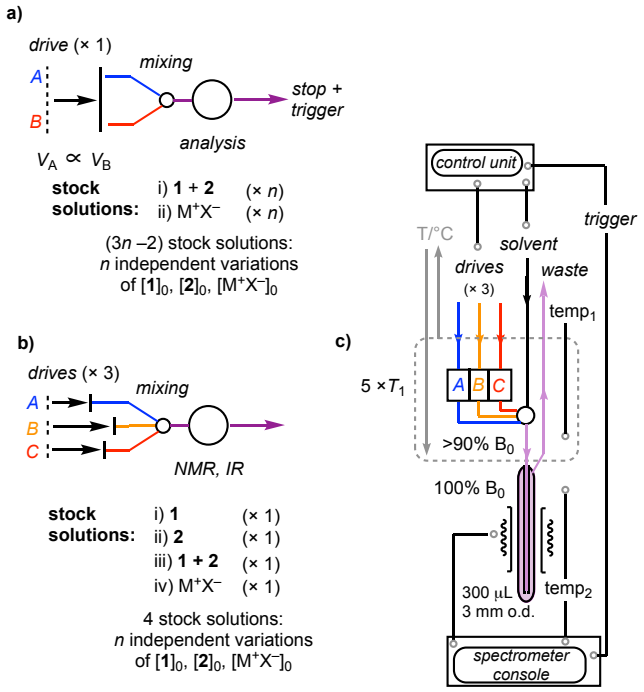

Figure 3. Schematic representations of: (**a**) classic fixed-ratio dual input stopped-flow; (**b**) a variable-ratio triple-input design; (**c**) variable-ratio stopped-flow NMR with thermostatic pre-magnetization of reactants (*A*,*B*,*C*), for >5 × T_1 at >90% (B_0).

To address this issue, we constructed a stopped-flow system, in which the delivered volumes of *three* solutions (*A*, *B*, *C*) are independently variable,[55] using a computer-controlled triple stepper-motor system, Figure 3b. This set-up allowed systematic analysis of the kinetics across a wide range of initial conditions, *using just four stock solutions*: mixing {i + iii + iv} varies [**2**]$_0$; mixing {ii + iii + iv} varies [**1**]$_0$; and mixing {iii + iv + THF} varies [M^+X^-]$_0$, whilst keeping the other species constant; see SI for full details. The new system was implemented in two modes: IR and NMR.[56] The former simply required adaptation of our recently developed thermostatted ATR-FTIR stopped-flow cell,[57] replacing the dual mixing stage with a triple mixer and a gated reaction volume. The analogous set-up for variable ratio stopped-flow NMR[56a] required bespoke construction. The principles for continuous-flow NMR recently reported by Foley *et al*.[58] were employed for the basic design, such that the reaction vessel and associated components can be installed simply by insertion of the device into the sample transit of a standard unmodified NMR spectrometer. Nuclei pre-magnetization is facilitated in three independent reservoirs (*A, B, C*) located as close as possible to the magnetic field center, Figure 3c. The reservoirs connect at a tripodal-geometry mixer that discharges via a 0.5 mm i.d. glass capillary into a 3 mm external diameter 300 µL glass NMR flow-cell. The tube terminates at the base of the cell, with the waste outlet at the top. A fourth input to the mixer allows the system to be flushed with solvent between runs. Thermostatting is achieved by passage of a heat-transfer medium (aq. ethylene glycol), using an externally controlled recirculator, through an umbilical containing all stages of the stopped-flow circuit, except for the glass flow-cell which is located within the spectrometer-thermostatted probe head; precalibration ensures $temp_1$ = $temp_2$. During a typical stopped-flow 'shot', a total of 600 µL is delivered through the flow-cell at a rate of 1–2 mL s^{-1}, fully displacing the previous contents and replacing it with 300 µL of freshly-assembled reaction mixture; charging requires 70-130 msec (measured independently by UV-Vis), with high quality NMR spectra (N_2-cryoprobe) achievable immediately thereafter. Control of the timing of the NMR pulse sequence is achieved by a trigger-signal, sent to the spectrometer console from the computer-controlled triple stepper-motor system, immediately after the 300 µL flow-cell has been freshly charged.

7. Kinetics of Trifluoromethylation by $TMSCF_3$ (1a) and $TIPSCF_3$ (1c) The kinetics of reactions initiated by M^+X^-, where M^+ = Bu_4N^+, K^+, and Cs^+, were studied in detail by SF-IR and SF-NMR across a wide range of concentrations of **1a**, **2** and [M^+X^-]$_0$. For FTIR, the decay in the IR C-F stretching mode (1056 cm^{-1}) of the $TMSCF_3$ (**1a**) and the growth in C–F stretching mode (1165 cm^{-1}) of **3**$_{OTMS}$ were collected at scan-rates of 14 or 28 s^{-1} with a resolution of 2 or 8 cm^{-1}, respectively. ^{19}F NMR analysis allowed detailed analysis of the reaction components, but was naturally more-limited in terms of temporal resolution. For faster reactions, a technique involving the interleaving of a series of spectra from a sequence of stopped-flow NMR 'shots' was employed, affording a higher virtual temporal resolution.

A key component in analysis of the kinetics was the dependence of the temporal-concentration evolution of the product (**3**$_{OTMS}$) on the concentration *ratio* of ketone **2** and $TMSCF_3$ (**1a**). Systematic studies of initial rates using TBAT led to an

empirical rate equation for turnover frequency (TOF) in which the initiator ($Bu_4N^+X^-$) and ketone **2** are first order, and the $TMSCF_3$ (**1a**) reagent approximately *inverse* first order (equation 1).[59] Control experiments in which the reactions were run in the presence of exogenous product (**3**$_{OTMS}$) confirmed that it does not act as an inhibitor.

$$\text{TOF} \approx \frac{k_{rxn}[M^+X^-]_0[\mathbf{2}]_t(1 - x_{EI})}{1 + K_{i1}[\mathbf{1}]_t} \approx k_{obs}\frac{[\mathbf{2}]}{[\mathbf{1}]} \quad \text{(eqn. 1)}$$

$$\text{TOF} \approx \frac{k_{rxn}[M^+X^-]_0[\mathbf{1}]_t(1 - x_{EI})}{1 + K_{i2}[\mathbf{2}]_t} \approx k_{obs}\frac{[\mathbf{1}]}{[\mathbf{2}]} \quad \text{(eqn. 2)}$$

The inhibitory effect of the $TMSCF_3$ reagent **1a** (K_{i1}; equation 1) results in very distinctive temporal concentration profiles for the reaction, simulations of which are presented later. For example, when the initial ratio of reactants is equal ($[\mathbf{2}]_0 = [\mathbf{1a}]_0$) their ratio remains constant ($[\mathbf{2}]_t/[\mathbf{1a}]_t = 1$) throughout the reaction. What arises is an apparent *pseudo* zero-order consumption of the reactants (TOF = k_{obs}) for the majority of the reaction evolution. Conversely, when there is an excess of ketone **2** over **1a** the rate of turnover rises as a function of conversion, becoming very rapid in the final phases of reaction where $[\mathbf{2}]_t/[\mathbf{1a}]_t >> 1$.

Systematic studies using M^+X^- (M^+ = Li^+, Na^+, K^+, Cs^+) which induce very rapid turnover, proved more challenging. Reactions where M^+ = Li^+, Na^+, stalled before completion and were not reproducible. KOPh and CsOPh initiated at very low concentrations, without an evident induction period, proceeded to completion, and provided reproducible kinetics. Study of the *initial* rates suggested higher-order dependencies on $TMSCF_3$ ($[\mathbf{1a}]_0$, again inverse) and on $[M^+X^-]_0$, with the ketone **2** remaining first-order. However, the reactions *evolve* with near-identical behaviour to those initiated by TBAT (equation 1).[59] The dichotomy is indicative of the presence of exogenous inhibitor(s) in low concentration in the $TMSCF_3$ (**1a**) reagent, that are not consumed during reaction. Increasing the initial concentration of the reagent ($[\mathbf{1a}]_0$), or decreasing the initiator concentration ($[M^+X^-]_0$), both cause a greater mol-fraction of exogeneous inhibition (x_{EI}), equation 1.[59,60] Addition of $[K]^+[(C_6F_5)_4B]^-$, to provide an additional soluble K^+ source with a non-nucleophilic counter-anion, had no impact on the kinetics of reactions initiated by KOPh, indicative that the rate is dependent on the initiating anion *concentration* and the counter-cation *identity* (but not its concentration).[61] Addition of potassium-binding ligands attenuated the rates substantially, and with crypt-222, the system underwent turnover slower than with Bu_4N^+ (a 3 orders of magnitude rate-reduction compared to free K^+).

The kinetics of trifluoromethylation of 4-fluorobenzaldehyde (**13**) by **1a** were also explored using TBAT as initiator. The aldehyde undergoes significantly faster trifluoromethylation than ketone **2** (k_{ald} / k_{ket} ≈ 80, at 21 °C) requiring lower initial TBAT concentrations, and causing the traces of exogeneous inhibitor(s) in **1a** to complicate the kinetics.[59] Competing ketone **2** with aldehyde **13** (9 / 1 ratio) using stopped-flow ^{19}F NMR to analyze the transient substrate ratio (**2**/**13**) during the first 5-30 seconds of reaction indicated that the relative rate of trifluoromethylation is independent of $[TBAT]_0$ (96–384 μM) and **1a** (0.08 to 0.48 M). Overall, the data is indicative that aldehyde **13** follows the same general kinetics as ketone **2**, i.e. equation 1.[59,60] The rate of trifluoromethylation of ketone **2** using $TIPSCF_3$ (**1c**) was much slower than with **1a**. Again, the kinetics were impacted by exogenous inhibitor(s) in the reagent ($[\mathbf{1c}]_0$), the effect of which (x_{EI}) varied from batch to batch of **1c**, see SI. Using TBAT as initiator, the reactions evolve with a first order dependency on the initiator, and on the reagent ($[\mathbf{1c}]_t$), with inhibition by the ketone (K_{i2}; equation 2). In other words, the kinetic dependencies are the opposite to that found for **1a** (compare equations 1 and 2) with reactions accelerating when there is an excess of **1c** over **2**. Reactions of **2** with **1c** initiated by KOPh were slower than those initiated by TBAT, and were accelerated on addition of crypt-222; the opposite phenomena to those observed with **1a**.

8. Stopped-Flow ^{19}F NMR Analysis of Siliconate and Alkoxide Intermediates, Exchange Dynamics with $TMSCF_3$, and Initiator Regeneration. By use of 4-F-benzophenone (**12**; δ_F −107.0 ppm), which reacts slower than **2**, and reducing the reaction temperature to 275 K, the temporal speciation of the initiator-derived species (10 mol% TBAT) was monitored using stopped-flow ^{19}F NMR, Figure 4. The known but unstable hypervalent bis-CF_3-siliconate (**D**; δ_F −63.3 ppm)[32-34] is generated instantly. Integration against fluorobenzene (internal standard, δ_F −113.2 ppm) shows **D** to be present at 10 mol%, and thus the predominant anion-speciation. A key feature in the time-series is the dynamic line-broadening in **D** that is constant throughout the reaction, but develops in the substoichiometric $TMSCF_3$ (**1a**) reagent (δ_F −66.6 ppm) as its concentration is depleted by the overall reaction with ketone **12**. In parallel with this is a marked acceleration in product generation (**14**$_{OTMS}$, δ_F −72.4 and −113.7 ppm), consistent with equation 1. After 6 seconds, the $TMSCF_3$ (**1a**) is fully consumed and TBAT (δ_F −97.4 ppm) is regenerated from Ph_3SiF / Me_3SiF. The dynamic-line broadening in **D** / **1a** can be satisfactorily simulated using a 3-spin exchange process in which **D** is in rapid dissociative equilibrium (k_{exch} ~180 s^{-1}; $\Delta G^‡$ ~13 kcal mol^{-1}) with **1a** and a low concentration of (unobserved) $[Bu_4N][CF_3]$ (**E**).[62] At 300 K, the line-broadening is very extensive and **D** short-lived.

Analogous experiments using $TIPSCF_3$ (**1c**) gave a very different outcome. Reactions conducted with **1c** at 275 K were slow enough to be followed using ketone **2** (δ_F −106.7 ppm), Figure 5. The ^{19}F NMR signal for **1c** remains sharp until **2** has been fully consumed. In contrast to reactions with **1a** (Figure 4) the alkoxide (**3**$_O$-; δ_F −118.4) is present in significant concentration and exhibits dynamic-line broadening (see inset to Figure 5). The signal for ketone **2**, also exhibits dynamic-line broadening, immediately after addition of the TBAT. On complete consumption of **2** (~120 s) the signals for remaining **1c** and CF_3H are broadened, presumably due to indirect exchange involving CF_3^-. After a further 300 s, **1c** is fully consumed and the CF_3H doublet becomes sharp again.

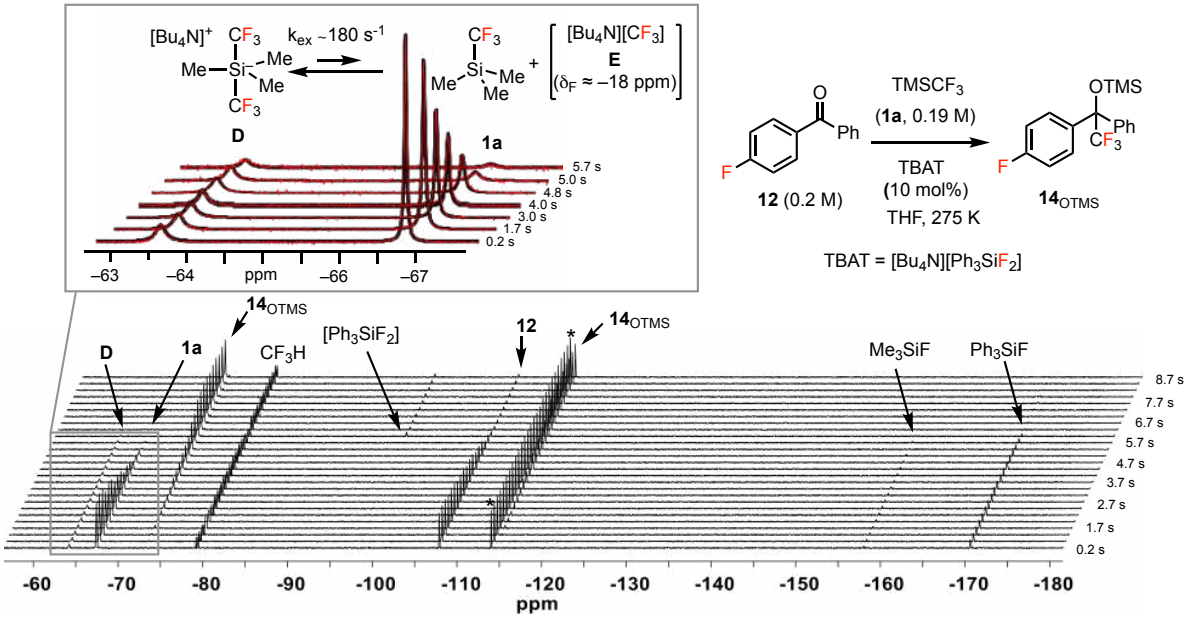

Figure 4. Selected spectra from stopped-flow ^{19}F NMR analysis of the reaction of 4-F-benzophenone **12** (0.20 M) with **1a** (0.19 M) in THF at 275 K after initiation by 10 mol% TBAT. Inset: overlay of selected simulations[62] (black) of dynamic line-shape for **D** / **1a** with experimental spectra (red); **E** (δ_F –18 ppm) is undetected. (*) C_6H_5F internal standard.

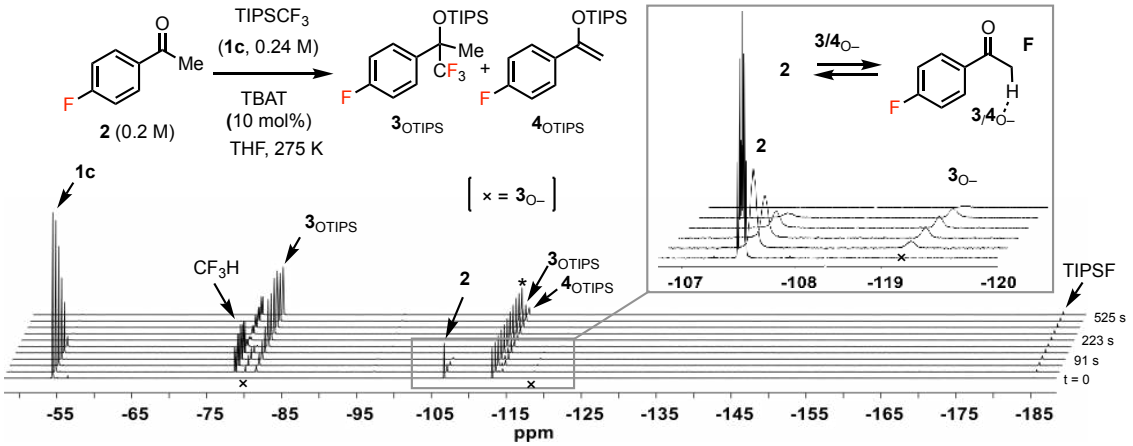

Figure 5. Selected spectra from *in situ* ^{19}F NMR analysis (manual assembly) of the reaction of 4-F-acetophenone **2** (0.20 M) with **1c** (0.2 M) in THF at 275 K after initiation by 10 mol% TBAT; (t = 0, no TBAT). Inset: line-broadening in ketone **2** and alkoxide $\mathbf{3}_{O-}$. (*) C_6H_5F internal standard. (x) = $\mathbf{3}_{O-}$. Free $\mathbf{4}_{O-}$ not located, possibly due to degenerate exchange with **2**. Ph_3SiF is not observed.

9. General Mechanism for Anion-initiated CF_3 Transfer from R_3SiCF_3 to Ketones and Aldehydes. The data outlined in Sections 2 to 8 above (see SI for full details) indicate that the M^+X^- initiated trifluoromethylation of ketone **2** by $TMSCF_3$ (**1a**) involves an electrophile-nucleophile reaction, in which the CF_3 transfer is accompanied by M^+. Enolsilane $\mathbf{4}_{OTMS}$ is also generated (≤ 2% when $M^+ = K^+$ and 7% when M^+ Bu_4N^+) with co-product CF_3H (k_H/k_D = 6.1). Using $TIPSCF_3$ (**1c**), approximately 50% of the product is $\mathbf{4}_{OTIPS}$ and k_H/k_D = 1.0. Contrasting kinetic behaviour is observed for **1a** (equation 1) versus **1c** (equation 2), with the roles of reactant for turnover, and inhibitor reversed between the two systems. These disparate sets of observations can easily be misinterpreted as turnover for **1a** versus **1c** arising from different pathways, e.g. siliconate versus carbanion. However, analysis of the kinetics, KIEs, and DFT calculations of a wide range of potential intermediates (see SI), eventually leads to the conclusion that the two reagents elicit contrasting kinetics, selectivity ($\mathbf{3}_{OSi}/\mathbf{4}_{OSi}$) and KIEs, by biasing one of two extremes in a single overarching mechanism. Calculations employed the M06L/6-31+G* level of theory, which was selected from a range of other functionals and larger basis sets that were considered,[63] see SI, as it provided the best quantitative agreement with experiment. All calculations were performed in Gaussian09,[64] with THF solvation incorporated via a PCM single point at the same level of theory, and with T = 298 K and pressure at 24.45 atm to achieve a 1 M standard state.[65] Kinetic isotope effects were computed using the Kinisot program.[66] Some of the TES and TIPS bearing structures required the 'loose' settings during the geometry optimization, presumably because of the flat potential energy surface associated with the long Si-CF_3 bonds.

The calculations permitted several possible structure types (such as hexacoordinate silicon dianions) to be excluded from consideration, and also revealed pronounced differences between intermediates based on TMS, TES, and TIPS,

where the increasing steric bulk substantially destabilizes the pentacoordinate anions, Figure 6. Extensive calculations were conducted to test for direct nucleophilic reactivity of the pentacoordinate anions **B** and **D**. All calculations revealed that *direct* transfer of CF_3 from the silicon centre to an electrophile requires concomitant inversion of the CF_3, with a prohibitively large barrier (>100 kcal mol^{-1}; in line with the barrier for inversion of the free CF_3 anion).[67] The pentacoordinate siliconate anions thus act as reservoirs, not active nucleophiles, liberating free (non-silicon coordinated) CF_3^- via dissociation. The transition state for addition of the CF_3^- anion(oid) to the ketone formally involves movement between a non-classical hydrogen bonded complex and the addition product, a process that occurs with low calculated barrier (7.5 kcal mol^{-1}) and well-represents the process that occurs once the two species are in contact. The calculations support the known preference for deprotonation (k_{CH}) in the gas phase,[68] and for addition (k_{CO}) once solvation is introduced, as observed experimentally for $TMSCF_3$ (**1a**). The loose addition transition state leads to a negligible ^{13}C KIE (carbonyl) for addition, while a large primary ^2H KIE is computed for C–H deprotonation. Relative rates computed from activation free energies suggest ρ = 2.0 for addition to acetophenones, and a lower barrier for addition to 4-F-benzaldehyde (**13**) versus **2** (ΔΔG‡ 2.6 kcal/mol; k_{rel} = 81). All of these computed values are in excellent agreement with experiment.

A general mechanism for the trifluoromethylation of ketones and aldehydes by R_3SiCF_3 reagents (**1**) in the presence of a catalytic quantity of initiator (M^+X^-) can thus be assembled, Figure 7. The one overarching mechanism, discussed below in the context of two extremes (V*i* and V*ii*), rationalizes why the turnover rate (per M^+X^- initiator) for a given electrophile depends on the initial concentration (but not identity) of X^-, the identity (but not concentration) of M^+, the identity of the reagent (**1a-c**), and the electrophile / reagent ratio (**2** / **1**).

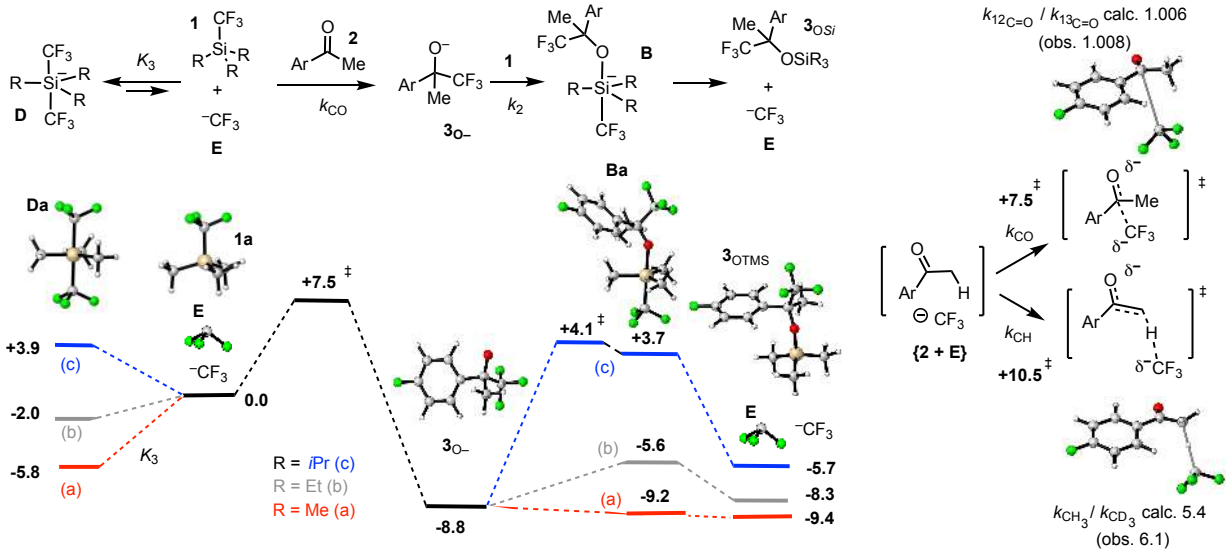

Figure 6. Selected structures and energies (M06L/6-31+G*; PCM (THF); standard state, 1 M; 298 K) of naked anions in the reaction of ketone **2** with R_3SiCF_3 **1a-c**. Energies have been normalized to [CF_3^- + **1** + **2**] = 0.00 kcal mol^{-1}. See text, Figure 9, and the SI for discussion of the binding modes and effects of cations. The structures and energies of other potential intermediates examined, including hexacoordinate dianions and fluoride adducts, are provided in the SI.

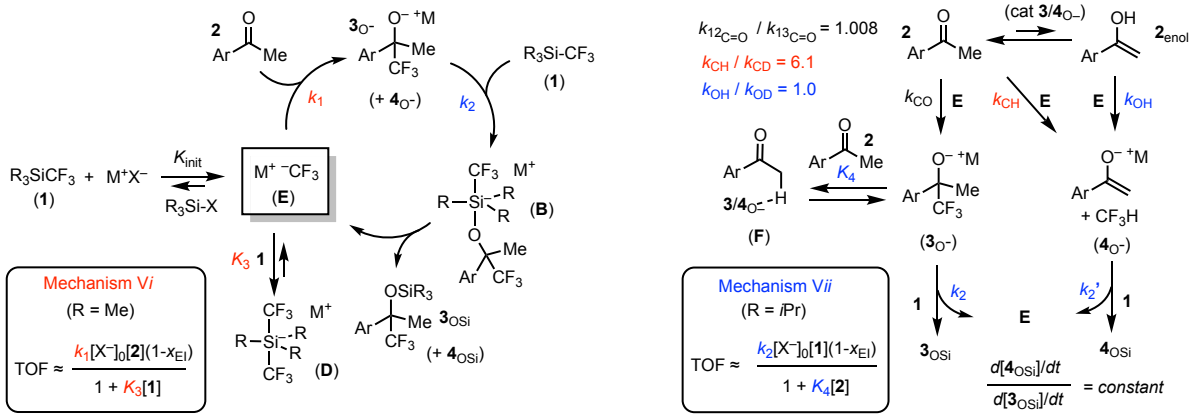

Figure 7. Mechanisms V*i* and V*ii*: two extremes of general model V for the trifluoromethylation of ketones by R_3SiCF_3 reagents **1a-1c**, in the presence of a catalytic quantity of initiator M^+X^-, with acetophenone as a generic reactant. Turnover frequency (TOF) equations are simplifications of a global approximation, where $k_1 = k_{CO} + k_{CH} + k_{OH}[\mathbf{2}_{enol}]/[\mathbf{2}]$, and the mol-fraction of active anion quenched by unidentified exogenous inhibitor(s) in **1**, is x_{EI}. Initiation (K_{init}) is not included in the rate equation. When M^+X^- is 'TBAT', initiation is reversible using **1a**. For non-enolizable ketones and aldehydes, k_{CH}, k_{OH}, and $K_4 = 0$.

10. Mechanism V*i*. In this regime, which describes reactions involving $TMSCF_3$ (**1a**), the dominant anion speciation is the bis(trifluoromethyl) siliconate (**D**),[32-34] generated in rapid equilibrium (K_3) with CF_3^- (**E**)[36,38] and **1a**, as observed by NMR, Figure 4. The product-determining step (k_1) involves reaction of CF_3^- (**E**) with the ketone (**2**), ($k_{CO} + k_{CH}$), and the reagent (**1a**) thus acts as a reversible inhibitor. The stronger the association of M^+ with CF_3^- (see Section 13) and with the carbonyl oxygen, the faster the turnover rate: Bu_4N^+ < [K(crypt-222)]$^+$ < [K(18-c-6)]$^+$ < K^+. The initial concentration *ratios* of the reactant versus the reagent dictate the temporal evolution of the reaction. When $[\mathbf{2}]_0/[\mathbf{1a}]_0 = 1$, *pseudo* zero order kinetics are obtained, whereas when $[\mathbf{2}]_0/[\mathbf{1a}]_0 \geq 1$ the rate rises throughout the reaction, becoming very fast (asymptoting to $k_{-3}[\mathbf{D}]$) in the final stages. The kinetics of trifluoromethylation of ketone **2** by $TMSCF_3$ (**1a**), can be satisfactorily simulated, Figure 8, using a truncated form of mechanism V*i* that retains relationships required for TOF modulation as the temporal concentration *ratio* $[\mathbf{2}]_t/[\mathbf{1a}]_t$ evolves.

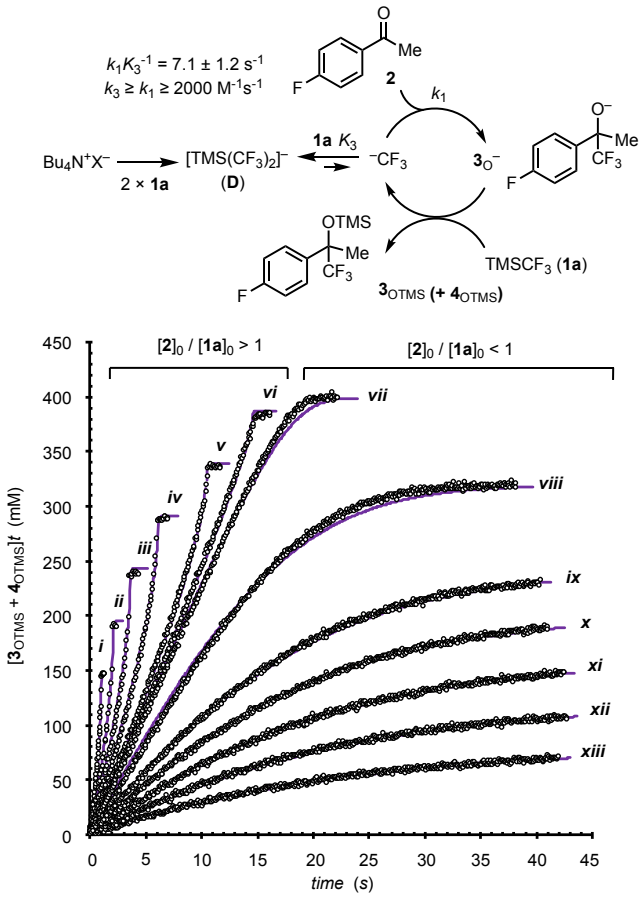

Figure 8. Simulation of experimental data (open circles, SFIR; $[\mathbf{3}_{OTMS} + \mathbf{4}_{OTMS}]_t$) based on simplified mechanism V*i*, for reaction of ketone **2** with $TMSCF_3$ (**1a**), initiated by 3.6 mM TBAT ($Bu_4N^+X^-$). For $[\mathbf{2}]_0/[\mathbf{1a}]_0$ >1, $[\mathbf{2}]_0$ = 0.40 M and $[\mathbf{1a}]_0$ = 144, 192, 248, 288, 336, 384 mM (i to vi). For $[\mathbf{2}]_0/[\mathbf{1a}]_0$ <1, $[\mathbf{1a}]_0$ = 0.48 M and $[\mathbf{2}]_0$ = 400, 320, 240, 200, 160, 120, 80 mM (vii to xiii). Induction and turnover by **1a** are set to arbitrary high values. Fitted parameters (k_1, k_3, k_{-3}) as indicated; $x_{EI} = 0.59$

11. Mechanism V*ii*. In this regime, which describes reactions involving $TIPSCF_3$ (**1c**), the dominant anion speciation is a combination of the product alkoxide ($\mathbf{3}_O$-), the enolate anion ($\mathbf{4}_O$-), and MX. Ketone (**2**) can reversibly H-bond (**F**) with oxy-anions **3**/$\mathbf{4}_O$-, as observed by NMR, Figure 5, leading to inhibition (K_4).[69] When $[\mathbf{1c}]_0/[\mathbf{2}]_0 = 1$ *pseudo* zero order kinetics are observed; reactions in which $[\mathbf{1c}]_0/[\mathbf{2}]_0$ >1 exhibit accelerating rate in the last stages of reaction. The more strongly bound M^+ to [**3**/$\mathbf{4}_O$-], the slower the reaction with **1c**, leading to rates increasing in the series: K^+ < [K(18-c-6)]$^+$ < Bu_4N^+ < [K(crypt-222)]$^+$; i.e. the opposite order to V*i*. When the non-enolizable ketone 4-F-benzophenone **12** is employed, the kinetics show clean pseudo first-order decay in **1c**, see SI, with no inhibition by **12** (i.e. Mechanism V*ii*, where $K_4 = 0$; and equation 2, where $K_{i2} = 0$).

12. Competing Enolization. Also shown in Figure 7 is the generation of the enol ether ($\mathbf{4}_{OSi}$) and CF_3H from ketone **2**, for which the selectivity ($\mathbf{4}_{OSi}$ / $\mathbf{3}_{OSi}$) is dependent on M^+ and the reagent (**1a-c**), Table 1. The major pathway for generation of $\mathbf{4}_{OTMS}$ in mechanism V*i* is via C–H deprotonation (k_{CH}) with an attendant large primary ^{2}H-KIE.[70,71] In contrast, for mechanism V*ii*, the significant concentration of [**3**/$\mathbf{4}_O$-] allows keto-enol equilibrium (pK_{enol} ~8)[72] in **2** to be approached, with attendant intermolecular scrambling of ^{2}H between ketone methyl groups. Deprotonation (k_{OH}) of the enol ($\mathbf{2}_{enol}$) is predicted (DFT) to be of very low barrier, and thus proceed with a negligible ^{2}H-KIE.[70] Despite their different origins (k_{CH} versus k_{OH}) mechanisms V*i*, and V*ii* both lead to $\mathbf{4}_{OSi}$ / $\mathbf{3}_{OSi}$ ratios that are independent of the concentration of reactants (**1**, **2**) and constant throughout reaction, Figure 2.

13. Cation-CF_3 Interactions. The interactions between the CF_3^- anion (free and Si-bound) and the counter-cations K^+ and Me_4N^+ (as a model for Bu_4N^+) were explored computationally, with multidentate CF_3 interactions found to be favored, e.g. Figure 9; see SI for details.

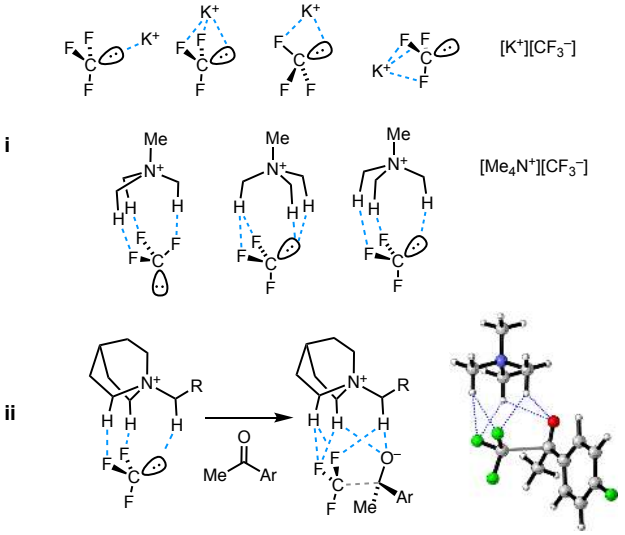

Figure 9. Cation binding to free CF_3 anion: (i) various modes of binding of K^+ and Me_4N^+ cations; (ii) concept (schematic) for enantioselective addition beneath the quinuclidinium core of a cinchonidinium initiator. Inset: structure of TS for addition of [CF_3^-][Me_4N^+] to **2**, see SI, with H-bonding interactions to developing alkoxide anion.

The *indirect* transfer of CF_3 from reagent **1a** to the ketone / aldehyde, i.e. via a silicon-free carbanion **E**, has implications

for the mode by which enantioselective catalysis can be achieved using chiral ammonium initiators, e.g. cinchonidinium salts. The CF_3-anion binding modes found computationally for Me_4N^+ (Figure 9i) show how an ammonium cation might simultaneously interact with a CF_3^- anion and control a developing alkoxide anion, Figure 9ii. Mechanism Vi contrasts most,[16de,31] but not all,[16f] prior interpretations, where mechanisms II/III (Scheme 2) involving CF_3-siliconates bearing the initiating (**C**) or propagating (**B**) anion, are proposed to play key roles in the enantioselective trifluoromethylation step.

14. Broader Mechanistic Aspects. The mechanistic features elucidated in the current study extend beyond carbonyl trifluoromethylation. A number of corollaries follow for generic anion-initiated trifluoromethylation of an electrophile (*E*) by **1a**, or deprotonation (R–H),[73] via pathways analogous to mechanism Vi, and where $[E, R–H]_0 >> [M^+X^-]_0$. Thus, the initiator (M^+X^-) affects the rate of reaction in a number of ways. $[X^-]_0$ sets the initial concentration of the siliconate ($[\mathbf{D}]_0 = (1\text{-}x_{EI})[X^-]_0$)[60] which, in the absence of endogenous inhibitors, is essentially constant throughout reaction. The insurmountable barrier for CF_3 inversion[67] means that, independent of the identity of the electrophile, *E*, or proton donor, R–H, the siliconate is unable to effect direct anionic trifluoromethyl transfer, Figure 10i. In all cases, the reaction must proceed via a dissociative pathway, Figure 10ii, in which M^+ plays a key role: the stronger the association of M^+ with CF_3 the more favourable k_{-3}. In contrast, efficient regeneration of the siliconate (k_2, Figure 7) is favored by weaker interactions between M^+ and the anionic co-product from trifluoromethyl transfer (CF_3–*E*$^-$; R$^-$; or products thereof). When the anion is unable to react with **1a**, stoichiometric initiation by $[M^+X^-]$ is required.[14-26]

15. Exogenous Inhibition. Trifluoromethylations initiated by low concentrations of (M^+X^-) are highly sensitive to traces of exogenous inhibitor(s). Species that generate of an anion (LG^-) of insufficient reactivity towards **1a** to propagate, will terminate the anionic chain reaction, Figure 10iii. In a series of control experiments, additives of the form Z-LG, (Z = H, R_3Si, LG = Cl, Br) were found to function as powerful inhibitors for the anion-initiated reaction of **2** with **1a**. For example, the trifluoromethylation of **2** (0.4 M) initiated by 150 μM TBAT ceases immediately on addition of 150 μM TMSCl, see SI. Slower-onset irreversible inhibition is effected by the more hindered TIPSCl, which is also inhibits the reaction of $TIPSCF_3$ (**1c**). Competing consumption of **1a** is effected by other species in low-concentrations, including CCl_4 (Cl-transfer),[74] Cl_3CH (deprotonation / Cl–transfer),[73b] and TMS-OH (deprotonation), but without significant chain termination. There was no detectable inhibition by DCE, CH_2Cl_2,[73b] TMS-O-TMS, Ph_3SiF, Me_3SiCF_2H, or MeCN.[73c]

In our experience, a diverse range of inhibitors, and competitors (e.g. CCl_4 and $CHCl_3$) are present, in low concentrations and variable proportions, in commercial samples of $TMSCF_3$ (**1a**). This leads to substantial differences in reaction outcome, depending on the supplier. For example, comparison of the reaction of **2** (0.40 M) with five samples of freshly-distilled **1a** (0.48 M) revealed that the concentration of initiator (TBAT, KOPh) required to effect >99% conversion of **2** ranged from 30 μM to 2.0 mM (0.0075 to 0.5 mol%); see SI.

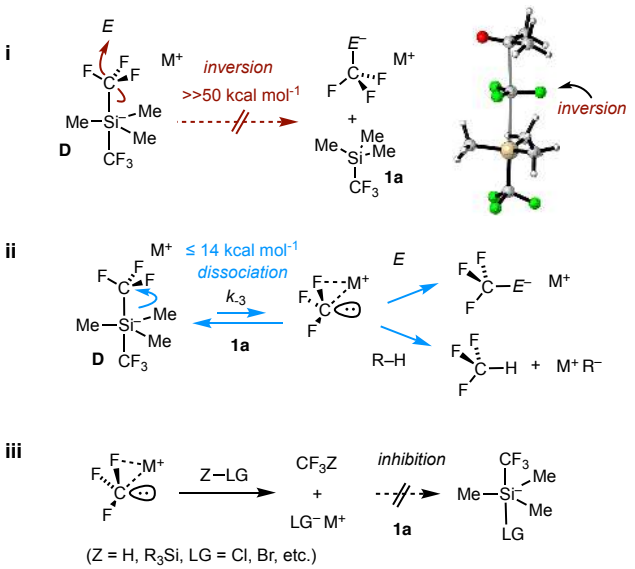

Figure 10. Generic reactivity of siliconate **D** towards electrophiles (*E*), carbon acids (R–H), and inhibitors (Z–LG). (i) *direct* CF_3 transfer from **D** is strongly disfavoured. Inset: TS for CF_3-transfer to acetone, see SI; (ii) dissociative CF_3 transfer, without CF_3 inversion; (iii) termination of the anionic chain reaction by traces of exogenous inhibitor(s), or substrates that generate an unreactive anion, LG^-.

An major difference found between reactions involving reagent **1a** versus **1b**,**c** is the impact of the persistent radical, TEMPO, which powerfully inhibits reactions involving **1a**, Scheme 4A. The difference in behavior towards TEMPO cannot arise from oxidation of the CF_3 anion (**E**), as this is a common intermediate to all three reagents (**1a-c**), and the partitioning of **E** between reaction with the ketone (**2**) versus TEMPO will be constant across the series, i.e. *independent* of the provenance of the carbanion **E**. Since the major difference between reagents **1a** and **1c** under the conditions of the reaction, is the dominant anion speciation (**D**; mechanism V*i*, **1a**, versus alkoxides **3**$_O^-$ / **4**$_O^-$; mechanism V*ii*, **1c**), this suggests that reaction of siliconate **D** with TEMPO is responsible for the inhibition. We were unable to identify any products *in situ*, or by quenching, arising from TEMPO under the standard reaction conditions, see SI. Whilst siliconates of type **D** are also generated from **1b** and **1c**, they are a) only present as low concentration or transient species, thus reducing their net rate of reaction with TEMPO, and b) may be more resistant to reaction with TEMPO due to their greater steric bulk.

CONCLUSIONS

The trifluoromethylation of ketones and aldehydes by $TMSCF_3$ (**1a**), initiated by catalytic fluoride ion, has been employed in synthesis for three decades.[12] Previous mechanistic work has focussed on stoichiometric reactions of R_3SiCF_3 (**1a,c**) with anions at low temperatures, generating unstable trifluoromethyl siliconates (**C**,**D**)[32-34] and carbanion(oids) (**E**),[36-38] depending on conditions. Which of these two pathways is followed in catalytic reactions at ambient temperature has been a long-standing mechanistic dichotomy.[30] A

variable-ratio stopped-flow NMR/IR approach (Figure 3) has been developed to facilitate time- and material-efficient analysis of a wide range of initiator (M^+X^-) and reactant concentrations. Change of reagent from $TMSCF_3$ (**1a**) to $TIPSCF_3$ (**1c**) has a profound impact on the reaction. For example, the conversion of 4-F-acetophenone (**2**, 0.4 M) to $\mathbf{3}_{OTMS}$ by equimolar **1a** in THF at ambient temperature takes < 125 msec to complete using 0.1 mol% KOPh initiator, and generates <2% of silylenol ether $\mathbf{4}_{OTMS}$, whereas with $TIPSCF_3$ (**1c**) and 3.75 mol% KOPh, the reaction proceeds to just 60% conversion in 16 hours, and generates 50% $\mathbf{4}_{OTIPS}$. The rates of reaction are strongly affected by traces of inhibitors present in the reagents (**1**), especially at the low concentrations of initiator (M^+X^-) employed for the fastest reacting systems, see equations 1 and 2.[59,60] Nonetheless, whilst these render initial rate data misleading, study of the full reaction time-course, e.g. Figure 8, provides a coherent kinetics analysis.

A unified mechanism (V) for the reaction of R_3SiCF_3 reagents (**1a-c**) with ketones and aldehydes under conditions of catalytic anionic initiator (M^+X^-) is presented in Figure 7. The work confirms that the carbanion[36-38] mechanism prevails under conditions of application (Scheme 1). Mechanism V allows a number of initially confusing observations to be rationalized. The main difference between use of $TMSCF_3$ (**1a**) versus $TIPSCF_3$ (**1c**) reagents is an inversion in the major anion speciation in the overall anionic chain reaction. This inversion leads to opposing influences of electrophile and silicon reagent (mechanisms V*i* and V*ii*), and to keto-enol equilibration (**2** / $\mathbf{2}_{enol}$) with **1c** (V*ii*). When TBAT is used as initiator,[75] $TESCF_3$ (**1b**) effects the most rapid trifluoromethylation in the series **1a-c**. The increased steric bulk in **1b** reduces reagent inhibition (K_3) relative to **1a**, without the substantial kinetic penalty in k_2 experienced by **1c**. These factors shift the reaction with **1b** closer to an 'ideal' catalytic cycle in which the intermediates are all connected by low TS barriers, with reduced off-cycle speciation. A consequence of adding $TMSCF_3$ (**1a**) to $TESCF_3$ (**1b**) is therefore to strongly inhibit turnover of **1b** until all of **1a** has been consumed, Figure 1.

The overarching mechanism (V, Figure 7) for anion-initiated reactions of R_3SiCF_3 (**1**) with ketones and aldehydes should prove of utility in their application in synthesis. For example, in the context of the design and analysis of enantioselective trifluoromethylation processes,[16,29,30a,31] mechanism V shows that control must be achieved by the CF_3^- / $[M]^+$ ion pair, Figure 9ii, and not by a siliconate intermediate. Moreover, the key mechanistic features of the anion-initiated reactions of **1** with carbonyl compounds (Figure 7) translate to reactions of **1** with other electrophiles (*E*),[29-31] and proton donors (R–H to generate R^-),[73] Figure 10. Thus, all processes in which siliconate **D** or analogous species, formally acts as a nucleophilic or basic source of CF_3, must proceed via a dissociative pathway (Figure 10ii). Siliconate **D** is inherently unstable, and decomposes at ambient temperature to generate, inter alia, complex perfluorocarbanions.[34,38a] The rate of anionic chain transfer, as dictated by the reactivity of the electrophile (*E*)[29-31] or carbon acid (R-H)[73] towards CF_3^-, as well as the presence of species able to attenuate decomposition (e.g. via CF_2-capture, $\mathbf{4}_{OSi} \rightarrow \mathbf{10}$, Scheme 3), controls the formal lifetime of **D**, and in turn the minimum loading of initiator (M^+X^-) that will be required to achieve complete conversion of substrate. Moreover, traces of exogenous inhibitor(s), (e.g. Z–LG, Figure 10iii) ubiquitous in R_3SiCF_3 reagents (**1**), act to reduce the net active anion in the chain reaction, again increasing the requisite loading of initiator (M^+X^-). Compounds employed in synthetic routes to reagents **1a-c**, e.g. TMSCl and TIPSCl,[11] function as powerful inhibitors. However, the identity and effect of the inhibitors in reagents **1a-c** vary substantially from batch to batch, and between commercial suppliers (see SI). Electrophiles or carbon acids (R–H) that react with CF_3^- to ultimately generate an anion of inherently low reactivity towards **1**, require stoichiometric initiator to proceed to completion.[14-26]

ASSOCIATED CONTENT

Supporting Information: Additional discussion, experimental procedures, further kinetic data and analysis, characterization data and NMR spectra. This material is available free of charge via the Internet at http://pubs.acs.org.

AUTHOR INFORMATION

Corresponding Author

Guy.lloyd-jones@ed.ac.uk

Author contributions

∫ C.P.J. and T.H.W. contributed equally to this work.

Notes

The authors declare no competing financial interest.

Funding Sources

The research leading to these results has received funding from the European Research Council under the European Union's Seventh Framework Programme (FP7/2007-2013) / ERC grant agreement n° [340163]. The Carnegie Trust provided a collaborative research grant. C.P.J. thanks the EC for an International Outgoing Fellowship (PIOF-GA-2013-627695).

ACKNOWLEDGMENT

We thank Veronica Forcina (Edinburgh, UK) and Prof. Dusan Uhrin (Edinburgh, UK) for assistance with stopped-flow NMR and dynamics, and Dr Per-Ola Norrby (AstraZeneca, Sweden) for valuable mechanistic discussions in the early phases of this work.

REFERENCES

(1) Selected reviews: a) Purser, S.; Moore, P. R.; Swallow, S.; Gouverneur, V. Fluorine in medicinal chemistry. *Chem. Soc. Rev.* **2008**, *37*, 320-330; b) Gillis, E. P.; Eastman, K. J.; Hill, M. D.; Donnelly, D. J.; Meanwell, N. A. Applications of Fluorine in Medicinal Chemistry. *J. Med. Chem.* **2015**, *58*, 8315–8359; c) Zhou, Y.; Wang, J.; Gu, Z.; Wang, S.; Zhu, W.; Aceña, J. L.; Soloshonok, V. A.; Izawa, K.; Liu, H. Next Generation

of Fluorine-Containing Pharmaceuticals, Compounds Currently in Phase II–III Clinical Trials of Major Pharmaceutical Companies: New Structural Trends and Therapeutic Areas. *Chem Rev*. **2016**, *116*, 422–518.

(2) Selected recent reviews: a) Fujiwara, T.; O'Hagan, D. Successful fluorine-containing herbicide agrochemicals. *J. Fluor. Chem*. **2014**, *167*, 16–29. b) Jeschke, P. The unique role of halogen substituents in the design of modern agrochemicals. *Pest. Manag. Sci.* **2010**, *66*, 10–27.

(3) Babudri, F.; Farinola, G. M.; Naso, F.; Ragni, R. Fluorinated organic materials for electronic and optoelectronic applications: the role of the fluorine atom. *Chem. Commun.* **2007**, 1003–1022.

(4) Berger, R.; Resnati, G; Metrangolo, P.; Weber, E.; Hulliger, J. Organic fluorine compounds: a great opportunity for enhanced materials properties. *Chem. Soc. Rev.* **2011**, *40*, 3496–3508.

(5) *Fluorinated Polymers (Volumes 1 and 2)*; Ameduri, B.; Sawada, H., Ed.; Royal Society of Chemistry: Cambridge, U.K., 2017.

(6) Ni, C.; Hu, J. The unique fluorine effects in organic reactions: recent facts and insights into fluoroalkylations. *Chem. Soc. Rev*. **2016**, *45*, 5441–5454.

(7) Vincent, J. M. Fluorous Catalysis: From the Origin to Recent Advances. *Top. Curr. Chem*., **2012**, *308*, 153–174**.**

(8) Langlois, B. R.; Billard, T.; Roussel, S. Nucleophilic trifluoromethylation: Some recent reagents and their stereoselective aspects. *J. Fluor. Chem.* **2005**, *126*, 173–179.

(9) See for example : a) Zhang, Y.; Fujiu, M.; Serizawa, H.; Mikami, K. Organocatalysis approach to trifluoromethylation with fluoroform. *J. Fluor. Chem.* **2013**, *156*, 367–371; b) Musio, B.; Gala, E.; Ley, S. V. Real-Time Spectroscopic Analysis Enabling Quantitative and Safe Consumption of Fluoroform during Nucleophilic Trifluoromethylation in Flow. *ACS Sustainable Chem. Eng.* **2018**, *6*, 1489−1495.

(10) a) Geri, J. B.; Szymczak, N. K. Recyclable Trifluoromethylation Reagents from Fluoroform. *J. Am. Chem. Soc.* **2017**, *139*, 9811−9814; b) Geri, J. B.; Wade Wolfe, M. M.; Szymczak, N. K. Borazine-CF_3^-Adducts for Rapid, Room Temperature, and Broad Scope Trifluoromethylation. *Angew. Chem. Int. Ed*. **2018**, *57*, 1381–1385.

(11) a) Ruppert, I.; Schlich, K., Volbach, W. Die Ersten CF_3-Substituierten Organyl(Chlor)Silane. *Tetrahedron Lett.* **1984**, *25*, 2195–2198. b) Ramaiah, P., Krishnamurti, R.; Prakash, G. K. S. 1-trifluoromethyl-1-cyclohexanol. *Org. Synth.* **1995**, *72*, 232–236; c) Prakash, G. K. S.; Jog, P. V.; Batamack, P. T. D.; Olah, G. A. Taming of Fluoroform: Direct Nucleophilic Trifluoromethylation of Si, B, S, and C Centers. *Science* **2012**, 1324–1327; d) Pawelke, G. Tetrakis(dimethylamino)ethylene/trifluoroiodomethane. a Specific Novel Trifluoromethylating agent. *J. Fluor. Chem*. **1989**, *42*, 429–433; e) Eaborn, C.; Griffiths, R. W.; Pidcock, A. Further Studies on Reactions of Organic Halides With Disilanes Catalysed by Transition Metal Complexes. *J. Organometal. Chem*. **1982**, *225*, 331–341.

(12) a) Kruse, A.; Siegemund, G.; Schumann, A.; Ruppert I., A process for the production of perfluoroalkyl compounds, and the pentafluoroethyl-trimethylsilane. German Pat. DE3805534 (1989); priority date 23rd February 1988.

(13) a) Prakash, G. K. S.; Krishnamurti, R.; Olah, G. A. Synthetic methods and reactions. 141. Fluoride-induced trifluoromethylation of carbonyl compounds with trifluoromethyltrimethylsilane (TMS-CF_3). A trifluoromethide equivalent. *J. Am. Chem. Soc.* **1989**, *111*, 393–395; see also: b) Stahly, G. P.; Bell, D. R. A New Method for Synthesis of Trifluoromethyl-Substituted Phenols and Anilines. *J. Org. Chem.* **1989**, *54*, 2873–2877; c) Dubuffet, T.; Sauvêtre, R.; Normant, J. F. Reaction Des Fluorosilyloxirannes Avec Les Electrophiles En Presence D'une Quantite Catalytique D'ion Fluorure .*Tetrahedron Lett.* **1988**, *29*, 5923–5924; and for analogous fluoride-initiated nucleophilic transfer of CF_2H, see d) Chen, D.; Ni, C.; Zhao, Y.; Cai, X.; Li, X.; Xiao, P.; Hu, J. Bis(difluoromethyl)trimethylsilicate Anion: A Key Intermediate in Nucleophilic Difluoromethylation of Enolizable Ketones with Me_3SiCF_2H. *Angew. Chem. Int. Ed.* **2016**, *55*, 12632–12636.

(14) a) Prakash, G. K. S., Yudin, A, K. Perfluoroalkylation with Organosilicon Reagents. *Chem Rev*. **1997**, *97*, 757–786. b) Singh, R. P.; Shreeve, J. M. Nucleophilic Trifluoromethylation Reactions of Organic Compounds with (Trifluoromethyl)trimethylsilane *Tetrahedron*, **2000**, *56*, 7613–7632; c) Gawronski, J.; Wascinska, N; Gajewy, J. Recent Progress in Lewis Base Activation and Control of Stereoselectivity in the Additions of Trimethylsilyl Nucleophiles. *Chem. Rev.* **2008**, *108*, 5227–5252.

(15) a) Singh, R. P.; Cao, G.; Kirchmeier, R. L.; Shreeve, J. M. Cesium Fluoride Catalyzed Trifluoromethylation of Esters, Aldehydes, and Ketones with (Trifluoromethyl)trimethylsilane. *J. Org. Chem.* **1999**, *64*, 2873–2876. b) Krishnamturi, R.; Bellew, D. R; Prakash, G. K. S. Preparation of trifluoromethyl and other perfluoroalkyl compounds with (perfluoroalkyl)trimethylsilanes. *J. Org. Chem.* **1991**, *56*, 984–989. c) Prakash, G. K. S.; Panja, C.; Vaghoo, H.; Surampudi, V.; Kultyshev, R.; Mandal, M; Rasul, G.; Mathew, T.; Olah, G. A. Facile Synthesis of TMS-Protected Trifluoromethylated Alcohols Using Trifluoromethyltrimethylsilane ($TMSCF_3$) and Various Nucleophilic Catalysts in DMF. *J. Org. Chem.* **2006**, *71*, 6806–6813.

(16) a) Mizuta, S.; Shibata, N.; Akiti, S.; Fujimoto, H.; Nakamura, S.; Toru, T. Cinchona Alkaloids/TMAF Combination-Catalyzed Nucleophilic Enantioselective Trifluoromethylation of Aryl Ketones. *Org. Lett.* **2007**, *9*, 3707–3710. b) Mizuta, S.; Shibata, N.; Hibino, M.; Nagano, S.; Nakamura, S.; Toru, T. Ammonium bromides/KF catalyzed trifluoromethylation of carbonyl compounds with (trifluoromethyl)trimethylsilane and its application in the enantioselective trifluoromethylation reaction. *Tetrahedron* **2007**, *63*, 8521–8528. c) Nagao, H.; Kawano, Y.; Mukaiyama, T. Enantioselective Trifluoromethylation of Ketones with (Trifluoromethyl)trimethylsilane Catalyzed by Chiral Quaternary Ammonium Phenoxides. *Bull. Chem. Soc. Jpn*. **2007**, *80*, 2406–2412. d) Hu, X.; Wang, J.; Wei, L.; Lin, L.; Liu, X.; Feng, X. Cinchona alkaloid-derived quaternary ammonium salt combined with NaH: a facile catalyst system for the asymmetric trifluoromethylation of ketones. *Tetrahedron Lett.* **2009**, *50*, 4378–4380. e) Zhao, H.; Qin, B.; Liu, X.; Feng, X. Enantioselective trifluoromethylation of aromatic aldehydes catalyzed by combinatorial catalysts. *Tetrahedron* **2007**, *63*, 2682–2686. f) Caron, S.; Do, N. M.; Arpin, P.; Larivee, A. Enantioselective

Addition of a Trifluoromethyl Anion to Aryl Ketones and Aldehydes. *Synthesis*, **2003**, 1693–1698; g) Kawai, H.; Mizuta, S.; Tokunaga, E.; Shibata, N. Cinchona alkaloid/TMAF combination: Enantioselective trifluoromethylation of aryl aldehydes. *J. Fluorine Chem.* **2013**, *152*, 46–50; h) Okusu, S.; Hirano, K.; Yasuda, Y.; Tokunaga, E.; Shibata, N. Flow Trifluoromethylation of Carbonyl Compounds by Ruppert–Prakash Reagent and its Application for Pharmaceuticals, Efavirenz and HSD-016. *RSC Adv.*, **2016**, *6*, 82716–82720.

(17) For example, a substructure search on 14/06/2018 for the addition of $TMSCF_3$ (**1a**, exact reagent) to C=O (any carbonyl) -> C(OA)-CF_3 (A= any atom) using Reaxys / SciFinder gave 434/450 primary research papers and 631/811 patents.

(18) Dilman, A. D.; Levin, V.V. Nucleophilic Trifluoromethylation of C=N Bonds. *Eur. J. Org. Chem.* **2011**, 831–841.

(19) a) Jin, G; Zhang, X.; Fu, D; Dai, W.; Cao, S. Mild and metal-free trifluoromethylation and pentafluoroethylation of gem-difluoroalkenes with $TMSCF_3$ and $TMSCF_2CF_3$. *Tetrahedron*, **2015**, *71*, 7892–7899. b) Ono, T. Synthesis of highly branched perfluoroolefins that are super-congested via multi-substitution of trifluoromethyl groups: Trifluoromethylation of hexafluoropropene trimers with Ruppert-Prakash reagent. *J. Fluor. Chem.* **2017**, *196*, 128–134.

(20) a) Furin, G. G.; Bardin, V. V. (Polyfluoroorganyl) trimethylsilanes in syntheses of fluoroorganic compounds. *J. Fluor. Chem.* **1991**, *54*, 241–241. b) Bardin, V. V.; Kolomeitsev, A. A.; Furin, G. G.; Yagupol'skii, Y. L. Trifluoromethylation of perfluoroaromatic compounds using trifluoromethyltrimethylsilane in the presence of fluoride ions. *B. Acad. Sci. USSR.* **1990**, *39*, 1539–1539.

(21) a) Kolomeitsev, A. A.; Movchun, V. N.; Kondratenko, N. V.; Yagupolski, Y. L. A Convenient Route to Aryl Trifluoromethyl Sulfones by Fluoride-Catalyzed Cross-Coupling of Arenesulfonyl Fluorides with (Trifluoromethyl)trimethylsilane and (Trifluoromethyl)trimethylstannane. *Synthesis*, **1990**, 1151-1152. b) Kowalczyk, R.; Edmunds, A. J.; Hall, R. G.; Bolm, C. Synthesis of CF_3-Substituted Sulfoximines from Sulfonimidoyl Fluorides. *Org. Lett*. **2011**, *13*, 768–771. c) Gouault-Bironneau, S.; Timoshenko, V. M.; Grellepois, F.; Portella, C. Thiophilic nucleophilic trifluoromethylation of α-substituted dithioesters. Access to S-trifluoromethyl ketene dithioacetals and their reactivity with electrophilic species. *J. Fluor. Chem.* **2012**, *134*, 164–171. d) Timoshenko, V. M.; Portella, C. Domino nucleophilic trifluoromethylations of alkyl perfluorodithioesters. *J. Fluor. Chem.* **2009**, *130*, 586–590. e) Yagupolskii, L. M.; Matsnev, A. V.; Orlova, R. K.; Deryabkin, B. G.; Yagupolskii, Y. L. A new method for the synthesis of trifluoromethylating agents—Diaryltrifluoromethylsulfonium salts. *J. Fluor. Chem*. **2008**, *129*, 131–136.

(22) a) Billard, T.; Langlois, B. R.; Large, S. Synthesis of Trifluoromethyl Selenides. *Phosphorus, Sulfur Silicon Relat. Elem.* **1998**, *136*, 521–524. b) Tyrra, W.; Naumann, D.; Yagupolskii, Y. L. Stable trifluoromethylselenates(0), [A]SeCF3—synthesis, characterizations and properties. *J. Fluor. Chem*. **2003**, *123*, 183–187.

(23) a) Tworowska, I.; Dabkowski, W.; Michalski, J. Synthesis of Tri- and Tetracoordinate Phosphorus Compounds Containing a PCF_3 Group by Nucleophilic Trifluoromethylation of the Corresponding PF Compounds. *Angew. Chem. Int. Ed.* **2001**, *40*, 2898–2900. b) Pane, P.; Naumann, D.; Hoge, B. Cyanide initiated perfluoroorganylations with perfluoroorgano silicon compounds. *J. Fluor. Chem*. **2001**, *112*, 283-286. c) Murphy-Jolly, M. B.; Lewis, L. C.; Caffyn, A. J. M. The synthesis of tris(perfluoroalkyl)phosphines. *Chem. Commun.* **2005**, 4479–4480.

(24) a) Molander, G. A.; Hoag, B. P. Improved Synthesis of Potassium (Trifluoromethyl)trifluoroborate [$K(CF_3BF_3)$]. *Organometallics* **2003**, *22*, 3313–3315. b) Kolomeitsev, A. A.; Kadyrov, A. A.; Szczepkowska-Sztolcman, J.; Milewska, M; Koroniak, H; Bissky, G.; Barten, J. A.; Röschenthaler, G.-V. Perfluoroalkyl borates and boronic esters: new promising partners for Suzuki and Petasis reactions. *Tetrahedron Lett.* **2003**, *44*, 8273–8277.

(25) Matousek,V.; Pietrasiak, E.; Schwenk, R.; Togni, A. One-Pot Synthesis of Hypervalent Iodine Reagents for Electrophilic Trifluoromethylation. *J. Org. Chem*. **2013**, *78*, 6763−6768**.**

(26) Tyrra, W.; Naumann, D.; Kirij, N. V.; Kolomeitsev, A. A.; Yagupolskii, Y. L. The first alkyl bismuthates: tris(trifluoromethyl)fluoro- and tetrakis(trifluoromethyl)-bismuthate. *J. Chem. Soc. Dalton Trans.* **1999**, 657–658.

(27) a) Prakash, G. K. S.; Krishnamoorthy, S.; Kar, S.; Olah, G. A. Direct S-difluoromethylation of thiols using the Ruppert–Prakash reagent. *J. Fluor. Chem.* **2015**, *180*, 186–191. b) Hashimoto, R.; Iida, T.; Aikawa, K.; Ito, S.; Mikami, K. Direct α-Siladifluoromethylation of Lithium Enolates with Ruppert-Prakash Reagent via C–F Bond Activation. *Chem. Eur. J.* **2014**, *20*, 2750–2754. c) Ito, S.; Kato, N.; Mikami, K. Stable (sila)difluoromethylboranes via C–F activation of fluoroform derivatives. *Chem. Commun.* **2017**, *53*, 5546–5548.

(28) Ni, C.; Hu, J. Recent Advances in the Synthetic Application of Difluorocarbene. *Synthesis*, **2014**, *46*, 842–863.

(29) a) Liu, X.; Xu. C.; Wang, M.; Liu, Q. Trifluoromethyltrimethylsilane: Nucleophilic Trifluoromethylation and Beyond. *Chem. Rev*. **2015**, *115*, 683-730; b) Takeshi Komiyama, T.; Minami, Y.; Hiyama, T. Recent Advances in Transition-Metal-Catalyzed Synthetic Transformations of Organosilicon Reagents. *ACS Catal*. **2017**, *7*, 631−651.

(30) a) Denmark, S. E.; Buetner, G. L. Lewis Base Catalysis in Organic Synthesis. *Angew. Chem. Int. Ed.* **2008**, *47*, 1560–1638; b) Reich, H. J. Mechanism of C-Si Bond Cleavage Using Lewis Bases (n→σ*). In *Lewis Base Catalysis in Organic Synthesis*, 1st ed.; Vedejs, E.; Denmark, S. E., Ed.; Wiley VCH: Weinheim, Germany, 2016; Volume 1, pp 251–253.

(31) For leading references see: a) Yang, X.; Wu, T.; Phipps, R. J.; Toste, F. D. Advances in Catalytic Enantioselective Fluorination, Mono-, Di-, and Trifluoromethylation, and Trifluoromethylthiolation Reactions. *Chem. Rev*. **2015**, *115*, 826–870; b) Shibata, N.; Mizuta, S.; Kawai, H. Recent advances in enantioselective trifluoromethylation reactions. *Tetrahedron: Asymmetry*, **2008**, *19* 2633–2644.

(32) Maggiarosa, N.; Tyrra, W.; Naumann, D.; Kirij, N. V.; Yagupolskii, Y. L. $Me_3Si(CF_3)F]^-$ and $[Me_3Si(CF_3)_2]^-$: Reactive Intermediates in Fluoride-Initiated Trifluoromethylation with Me_3SiCF_3 – An NMR Study. *Angew. Chem. Int. Ed.* **1999**, *38*, 2252–2253.

(33) Kolomeitsev, A.; Bissky, G; Lork, E.; Movchun, V.; Rusanov, E.; Kirsch, P.; Röschenthaler, G.-V. Different fluoride anion sources and (trifluoromethyl)trimethylsilane: molecular structure of tris(dimethylamino)sulfonium bis(trifluoromethyl)trimethylsiliconate, the first isolated pentacoordinate silicon species with five Si–C bonds. *Chem. Commun.* **1999**, 1017–1018.

(34) Tyrra, W.; Kremlev,M. M.; Naumann, D.; Scherer, H.; Schmidt, H.; Hoge, B.; Pantenburg, I. Yagupolskii, Y L. How Trimethyl(trifluoromethyl)silane Reacts with Itself in the Presence of Naked Fluoride—A One-Pot Synthesis of Bis([15]crown-5)cesium 1,1,1,3,5,5,5-Heptafluoro-2,4-bis(trifluoromethyl)pentenide. *Chem. Eur. J.* **2005**, *11*, 6514–6518.

(35) Kotun, S. P.; Anderson, J. D. O.; DesMarteau, D. D. Fluorinated Tertiary Alcohols and Alkoxides from Nucleophilic Trifluoromethylation of Carbonyl Compounds. *J. Org. Chem.* **1992**, *57*, 1124–1131.

(36) Prakash, G. K. S.; Wang, F.; Zhang, Z.; Haiges, R; Rahm, M.; Christe, K. O.; Mathew, T.; Olah, G. A. Long-Lived Trifluoromethanide Anion: A Key Intermediate in Nucleophilic Trifluoromethylations. *Angew. Chem. Int. Ed.* **2014**, *53*, 11575–11578.

(37) Santschi N.; Gilmour, R. The (Not So) Ephemeral Trifluoromethanide Anion. *Angew. Chem. Int. Ed.* **2014**, *53*, 11414–11415.

(38) a) Lishchynskyi, A.; Miloserdov, F. M.; Martin, E.; Benet-Buchholz, J.; Escudero-Adán, E. C.; Konovalov, A. I.; Grushin, V. V. The Trifluoromethyl Anion. *Angew. Chem. Int. Ed.* **2015**, *54*, 15289–15293; b) Miloserdov, F. M.; Konovalov, A. I.; Martin, E.; Benet-Buchholz, J.; Escudero-Adán, E. C.; Lishchynskyi, A.; Grushin, V. V. The Trifluoromethyl Anion: Evidence for $[K(crypt\text{-}222)]^+CF_3^-$. *Helv. Chim. Acta* **2017**, *100*, e1700032. c) Harlow, R. L.; Benet-Buchholz, J.; Miloserdov, F. M.; Konovalov, A. I.; Marshall, W. J.; Martin, E.; Benet-Buchholz, J.; Escudero-Adán, E. C.; Martin, E.; Lishchynskyi, A.; Grushin, V. V. On the Structure of $[K(crypt\text{-}222)]^+CF_3^-$. *Helv. Chim. Acta* **2018**, *101*, e1800015.

(39) The X-ray structural analysis of **E** (reference 38a) was challenged: Becker, S.; Müller, P. On the Crystal Structure Analysis of $[K(crypt\text{-}222)]^+CF_3^-$ a Reinterpretation: No Proof for the Trifluoromethanide Ion. *Chem. Eur. J.* **2017**, *23*, 7081–7086. The original interpretation was comprehensively defended, see reference 38c.

(40) The CF_3H contained traces of CF_3D (0.1 % ^{19}F NMR) likely from adventitious DOH / D_2O in the d_8-THF.

(41) Song, X.; Chang, J.; Zhu,D.; Li, J.; Xu, C.; Liu, Q.; Wang M. Catalytic Domino Reaction of Ketones/Aldehydes with Me_3SiCF_2Br for the Synthesis of α-Fluoroenones/α-Fluoroenals. *Org. Lett.* **2015**, *17*, 1712–1715.

(42) Song, X.; Xu, C.; Du, D.; Zhao, Z.; Zhu. D.; Wang M. Ring-Opening Diarylation of Siloxydifluorocyclopropanes by Ag(I) Catalysis: Stereoselective Construction of 2-Fluoroallylic Scaffold. *Org. Lett.* **2017**, *19*, 6542–6545.

(43) Pilcher, A. S.; DeShong, P. Utilization of Tetrabutylammonium Triphenyldifluorosilicate as a Fluoride Source for Silicon–Carbon Bond Cleavage. *J. Org. Chem.* **1996**, *61*, 6901–6905.

(44) Water may be liberated from the NMR tube surface, the reagents (**1a**, **2**; freshly distilled); the TBAT (anhydrous solid; THF solutions prepared and stored in a glove box); or the THF (~8 ppm H_2O, Karl-Fischer titration).

(45) Turnover rates were only affected by the impact on $TMSCF_3$/ketone ratio resulting from the rapid prior consumption of $TMSCF_3$ by the H_2O.

(46) For a review CF_3-transfer involving CF_3 radicals, see: Studer, A. A 'Renaissance' in Radical Trifluoromethylation. *Angew. Chem. Int. Ed.* **2012**, *51*, 8950–8958.

(47) For an example of CF_3 radical character transfer from $TMSCF_3$ via $AgCF_3$ intermediates, see Ye, Y.; Lee, S. H.; Sanford, M. S. Silver-Mediated Trifluoromethylation of Arenes Using $TMSCF_3$. *Org. Lett*. **2011**, *13*, 5464–5467**,** and references therein.

(48) Competing 1,4- and 1,6-addition to the aryl ring are characteristic of SET-type mechanisms for nucleophile addition to benzophenones; see: Holm, T.; Crossland, I. Mechanism of the Grignard Addition Reaction. *Acta. Chem. Scand.* **1971**, *25*, 59–69 and references therein.

(49) A near-continuum sequential SET pathway is possible; see e.g. Eisch, J. J. Single Electron Transfers in the Reactions of Carbanions. *Res. Chem. Interm.* **1996**, *22*, 145–187.

(50) a) Newcombe, M.; Johnson, C. C.; Manek, M. B.; Varick, T. R. Picosecond radical kinetics. Ring openings of phenyl-substituted cyclopropylcarbinyl radicals. *J. Am. Chem. Soc.* **1992**, *114*, 10915–10921. b) Miyazoe, H.; Yamago, S.; Yoshida, J. Novel Group-Transfer Three-Component Coupling of Silyltellurides, Carbonyl Compounds, and Isocyanides. *Angew. Chem. Int. Ed.* **2000**, *39*, 3669–3671.

(51) Biphenyl is significantly more stabilizing for radical pathways than 4-fluorophenyl ($\sigma C^{\bullet}$, +0.46, and –0.06 respectively), see: Creary, X. Super Radical Stabilizers. *Acc. Chem. Res*. **2006**, *39*, 761–771.

(52) For example, BuN^+X^- where X^- = $Ph_3SiF_2^-$, F^-, HO^-, PhO^-, and $\mathbf{3}_O^-$, behaved identically within experimental error. However when X^- was less nucleophilic, e.g. AcO^-, BzO^-, or 3,5-$(CF_3)C_6H_3O^-$, induction periods were evident. Induction periods were extreme with $KOC(CF_3)_3$.

(53) Luo, G.; Luo, Y.; Qu, J. Direct nucleophilic trifluoromethylation using fluoroform: a theoretical mechanistic investigation and insight into the effect of alkali metal cations. *New. J. Chem*. **2013**, *37*, 3274–3280.

(54) Control experiments confirmed that TBAT induces negligible H/D exchange between **2** and D_3-**2** over the reaction period, whereas $\mathbf{3}_{OK}$ induces complete scrambling in under 95 sec.

(55) For examples of mechanical variable ratio mixing for stopped-flow kinetics see: Goez, M. Inexpensive Pre-Mixer For Stopped-Flow Apparatus. *J. Phys. E: Sci. Instrum.* **1988**, *21*, 440–442, and references therein.

(56) For recent developments see: a) Dunn, A. L.; Landis, C. R. Progress toward reaction monitoring at variable temperatures: a new stopped-flow NMR probe design. *Magn. Reson. Chem*. **2017**, *55*, 329–336; b) Thomas, A. A.; Denmark, S. E. Ernest L. Eliel, a Physical Organic Chemist with the Right Tool for the Job: Rapid Injection Nuclear Magnetic Resonance. in *Stereochemistry and Global Connectivity: The Legacy of Ernest L. Eliel*, Cheng, H. N. Ed.; American Chemical Society, Washington DC, 2017; Volume 2, pp 105–134.

(57) Cox, P. A.; Reid, M.; Leach, A. G.; Campbell, A. D.; King, E. J.; Lloyd-Jones, G. C. Base-Catalyzed Aryl-B(OH)$_2$ Protodeboronation Revisited: From Concerted Proton Transfer to Liberation of a Transient Aryl Anion. *J. Am. Chem. Soc.* **2017**, *139*, 13156–13165.
(58) Foley, D. A.; Bez, E.; Codina, A.; Colson, K. L.; Fey, M.; Krull, R.; Piroli, D.; Zell, M. T.; Marquez, B. L. NMR Flow Tube for Online NMR Reaction Monitoring. *Anal. Chem.* **2014**, *86*, 12008–12013.
(59) Plots of initial rate versus [TBAT] for reaction of **2** and **13** with **1a** both have a non-zero *x*-axis intercept (0.03 mM) with curvature evident at low [TBAT] concentrations, see SI, suggesting the inhibitor(s) are present at <0.02% **1a**, in the specific batches of commercial reagents that were employed, see SI.
(60) In equations 1 and 2, and elsewhere, (1-x_{EI}) represents the mol-fraction of active anion relative to total anion [M^+X^-]$_0$. Based on a 1:1 inhibition mode, $x_{EI} = (K_{EI}[I]/(1+K_{EI}[I]))$ with $[I]_0 = x_i[\mathbf{1}]_0$, where x_i = mole fraction inhibitor in reagent **1**. Experimental data (see SI) suggest K_{EI} is substantially greater with **1c**.
(61) This contrasts the borazine systems recent developed by Szymczak (see ref 10) where addition of KBARF profoundly accelerates CF_3-transfer rates.
(62) Simulations were conducted using the three-spin parametrization in WNDNMR, with the rates and frequencies as indicated in Figure 4 ($k_{ex} = 2k_{ex}$; where k_{ex} is the apparent ^{19}F nuclei exchange rate through reassociation). The fraction of CF_3 present as **E** was arbitrarily set to 0.1%, with the remaining 99.9% partitioned between **D** and **1a** as required to fit. The chemical shift of CF_3[M] is reported as δ_F −18.7 ppm, see reference 38, and –17.2 ppm, see reference 36, depending on the identity of [M].
(63) Hariharan, P. C.; Pople, J. A. The influence of polarization functions on molecular orbital hydrogenation energies. *Theor. Chim. Acta* **1973**, *28*, 213–222.
(64) Gaussian 09, Frisch, M. J.; Trucks, G. W.; Schlegel, H. B.; Scuseria, G. E.; Robb, M. A.; Cheeseman, J. R.; Scalmani, G.; Barone, V.; Mennucci, B.; Petersson, G. A.; Nakatsuji, H.; Caricato, M.; Li, X.; Hratchian, H. P.; Izmaylov, A. F.; Bloino, J.; Zheng, G.; Sonnenberg, J. L.; Hada, M.; Ehara, M.; Toyota, K.; Fukuda, R.; Hasegawa, J.; Ishida, M.; Nakajima, T.; Honda, Y.; Kitao, O.; Nakai, H.; Vreven, T.; Montgomery, J. A., Jr.; Peralta, J. E.; Ogliaro, F.; Bearpark, M.; Heyd, J. J.; Brothers, E.; Kudin, K. N.; Staroverov, V. N.; Kobayashi, R.; Normand, J.; Raghavachari, K.; Rendell, A.; Burant, J. C.; Iyengar, S. S.; Tomasi, J.; Cossi, M.; Rega, N.; Millam, J. M.; Klene, M.; Knox, J. E.; Cross, J. B.; Bakken, V.; Adamo, C.; Jaramillo, J.; Gomperts, R.; Stratmann, R. E.; Yazyev, O.; Austin, A. J.; Cammi, R.; Pomelli, C.; Ochterski, J. W.; Martin, R. L.; Morokuma, K.; Zakrzewski, V. G.; Voth, G. A.; Salvador, P.; Dannenberg, J. J.; Dapprich, S.; Daniels, A. D.; Farkas, Ö.; Foresman, J. B.; Ortiz, J. V.; Cioslowski, J.; Fox, D. J. Gaussian, Inc., Wallingford CT, 2009.
(65) a) Zhao, Y.; Truhlar, D. G. The M06 suite of density functionals for main group thermochemistry, thermochemical kinetics, noncovalent interactions, excited states, and transition elements: two new functionals and systematic testing of four M06-class functionals and 12 other functionals. *Theor. Chem. Acc.* **2008**, *120*, 215–241. b) Zhao, Y.; Truhlar, D. G. Density Functionals with Broad Applicability in Chemistry. *Acc. Chem. Res.* **2008**, *41*, 157–167. c) Tomasi, J.; Mennucci, B.; Cammi, R. Quantum Mechanical Continuum Solvation Models. *Chem.Rev.* **2005**, *105*, 2999–3094.
(66) a) Brown, S. B.; Dewar, M. J. S.; Ford, G. P.; Nelson, D. J.; Rzepa, H. S. Ground states of molecules. 51. MNDO (modified neglect of diatomic overlap) calculations of kinetic isotope effects. *J. Am. Chem. Soc.* **1978**, *100*, 7832–7836. b) Dewar, M. J. S.; Olivella, S.; Rzepa, H. S. Ground states of molecules. 49. MINDO/3 study of the retro-Diels-Alder reaction of cyclohexene. *J. Am. Chem. Soc.* **1978**, *100*, 5650–5659. c) Rzepa, H. S. KINISOT. A basic program to calculate kinetic isotope effects using normal coordinate analysis of transition state and reactants., http://doi.org/10.5281/zenodo.19272, **2015**. d) Paton, R. S. Kinisot: v 1.0.0 public API for Kinisot.py. http://doi.org/10.5281/zenodo.60082, **2016**.
(67) Han, H.; Alday, B.; Shuman, N. S.; Wiens, J. P.; Troe, J.; Viggiano, A. A.; Guo, H. Calculations of the active mode and energetic barrier to electron attachment to CF_3 and comparison with kinetic modeling of experimental results. *Phys. Chem. Chem. Phys.* **2016**, *18*, 31064–31071.
(68) McDonald, R. N.; Chowdhury, A. K. Nucleophilic reactions of trifluoromethyl ion (F_3C-) at sp^2 and sp^3 carbon in the gas phase. Characterization of carbonyl addition adducts. *J. Am. Chem. Soc.* **1983**, *105*, 7267–7271.
(69) A range of anion-ketone interactions, including H-bonded adducts, aldolate products (see: Kolonko, K. J.; Reich, H. J. Stabilization of Ketone and Aldehyde Enols by Formation of Hydrogen Bonds to Phosphazene Enolates and Their Aldol Products. *J. Am. Chem. Soc.* **2008**, *130*, 9668–9669) and Diels-Alder product, as identities for inhibition by ketone **2**, were explored computationally, see SI. The lowest energy of these was an enolate-ketone H-bonded adduct (**F**).
(70) Thibblin, A.; Jencks, W. P. Unstable Carbanions. General Acid Catalysis of the Cleavage of 1-Phenylcyclopropanol and 1-Phenyl-2-arylcyclopropanol Anions. *J. Am. Chem. Soc.* **1979**, *101*, 4963–4973.
(71) The ^{2}H-KIE for α-CH deprotonation of d_3-**2** by LDA.LiOR is $k_H/k_D = 6.3$; with $(LDA)_2$ it is 1.7: Kolonko, K. J.; Wherrit, D. J.; Reich, H. J. Mechanistic Studies of the Lithium Enolate of 4-Fluoroacetophenone: Rapid-Injection NMR Study of Enolate Formation, Dynamics, and Aldol Reactivity. *J. Am. Chem. Soc.* **2011**, *133*, 16774–16777.
(72) Chiang, Y.; Kresge. A. J; Wirz, J. Flash-Photolytic Generation of Acetophenone Enol. The Keto-Enol Equilibrium Constant and p*K*a of Acetophenone in Aqueous Solution. *J. Am. Chem. Soc.* **1984**, *106*, 6392–6395.
(73) a) Sasaki, M.; Kondo, Y. Deprotonative C–H Silylation of Functionalized Arenes and Heteroarenes Using Trifluoromethyltrialkylsilane with Fluoride. *Org. Lett.* **2015**, *17*, 848–851; b) Behr, J.-B.; Chavaria, D.; Plantier-Royon, R. Trifluoromethide as a Strong Base: [CF_3^-] Mediates Dichloromethylation of Nitrones by Proton Abstraction from the Solvent. *J. Org. Chem.* **2013**, *78*, 11477–11482; c) Adams, D. J.; Clark, J. H.; Hansen, L. B.; Sanders, V. C.; Tavener, S. J. Reaction of Tetramethylammonium Fluoride with Trifluoromethyltrimethylsilane. *J. Fluor. Chem.* **1998**, *92*, 123–125; d) Yoshi-

matsu, M.; Kuribayashi, M. A Novel Utilization of Trifluoromethanide as a Base: a Convenient Synthesis of Trimethylsilylacetylene. *J. Chem. Soc., Perkin Trans. 1*, **2001**, 1256–1257; e) Nozawa-Kumada, K.; Osawa, S.; Sasaki, M.; Chataigner, I.; Shigeno, M.; Kondo. Y. Deprotonative Silylation of Aromatic C−H Bonds Mediated by a Combination of Trifluoromethyltrialkylsilane and Fluoride. *J. Org. Chem*. **2017**, *82*, 9487–9496.
(74) Zefirov, N. S.; Makhon'kov, D. I. X-Philic Reactions. *Chem. Rev.* **1982**, *82*, 615–624.

(75) The kinetics for reactions of **2** (0.4 M) with **1b** (0.48 M) are again complicated by inhibitors. When initiated by 0.3 mM KOPh the reaction is pseudo zero-order throughout; this result is consistent with a number of mechanisms, including for example turnover and inhibition by **1b**, or rate-limiting dissociation of CF_3 from dominant anion $\mathbf{B_b}$. The faster rates of reaction with Bu_4N^+ versus K^+ as counter-ion suggest mechanism V*ii* dominates.

GRAPHICAL ABSTRACT